Muséum national d'Histoire naturelle

International Erasmus Mundus Master in
QUATERNARY AND PREHISTORY

Erasmus Mundus

Old Breaks, New Takes: Diagnosing Trauma in the Anthropological Remains of Collège Claude Monet, Magny-en-Vexin, France (5th–7th Centuries CE)

Igor ROLLET

Tuteurs : Sébastien VILLOTTE, Frédéric BOURSIER, Jean-Gabriel PARIAT

Année académique 2024/2025

A mes grands-parents,

Pour tout ce que vous m'avez transmis
Pour votre amour, votre force,
Pour toujours avoir cru en moi,
Ce travail vous revient aussi.

Acknowledgments

I would like to thank Sébastien VILLOTTE, whose comments and guidance were invaluable, Frédéric BOURSIER for his trust and for sharing part of his knowledge, and Jean-Gabriel PARIAT for his help with the collection.

I am grateful to the *Service Départemental d'Archéologie du Val-d'Oise* for granting me access to its collection and for their warm welcome. I also extend my thanks to the radiology department of Gonnesse Hospital for their time and the genuine interest they dedicated to this research.

To my professors Dominique GRIMAUD-HERVÉ, Florent DETROIT, and Aline THOMAS: I hope that traces of your teaching can be found throughout this thesis. Thank you for sharing your knowledge and inspiring students like me.

To Marta AZARELLO, Julie ARNAUD, Anne-Marie SEMAH, François SEMAH, and Aldi LASSO: thank you for your support. It was a privilege to be your student and will carry many fond memories from this passionate master's program, stretching from France and Italy to Indonesia.

To Barbara BRAMANTI and Nicoletta ZEDDA: thank you for showing me what a supportive and inspiring laboratory environment can look like. Your teaching in paleopathology went far beyond methods and analysis, shaping my understanding of academic mentorship.

For their endless encouragement, many thanks to Wanda ZINGER, Lucie DEVILLIER, and Pierre GOUSSET.

To my peers: we were an incredible source of support during these past years. Léa DOERN, Inès CARRIERE, and Félicie BECK, our debates and your insights have been a guiding thread throughout this journey. Lou IGIER, Flore LUCAS, Noa LACHMAN, Léonard BOTTON, Juliette ELI, Maïwenn GOYAUX, Guillemette ETCHEGARAY, and Capucine FOURCHE made these two years far less depressing.

To my dear friends Emma GODDET, Emma FLANDI, Bleuwenn FERRANDON, Sanjay APAVOU, and Céline EKAMBI-POKOSSI, thank you for your support and your patience in enduring endless conversations about human remains. It was more than I could have hoped for.

Finally, to my family, thank you for raising me to think critically and for making the effort, more than once, to understand what exactly it is that I do.

Table of contents

List of Figures

List of Tables

Introduction

General context and rationale

The present research focuses on the human skeletal remains excavated in 1997-1998 from the Early Middle Ages necropolis under the site of the Collège Claude Monet in Magny-en-Vexin (Val-d'Oise, France). This burial ground partially excavated during early construction in 1972, comprises 62 documented inhumations dating from the 6th and 7th centuries CE. Located in the rural periphery of the Île de France region, the site reflects funerary practices associated with early medieval Christianized communities (Taupin et al. , 1998). The archeological context aligns with broader regional patterns identified by the PCR *Archéologie des nécropoles mérovingiennes d'Île-de-France,* which analyzed over 450 cemeteries to assess burial architecture, spatial organization, and socio-religious evolution during the transition from late antiquity to the Carolingian period (Le Forestier 2023).

Traumatic lesions preserved in skeletal remains offer unique insight into the lived experiences of past populations. As antemortem events, they often reflect patterns of insecurity broadly defined, from accidental injuries to acts of interpersonal or structural violence. Recent studies have emphasized both the cranial and postcranial manifestations of trauma (Baten and Steckel 2018) and their interpretative value for reconstructing living conditions and societal stressors (Dittmar et al. 2023). Yet, the complex nature of trauma requires a systematic and contextualized reading grid to ensure consistent identification and nuanced interpretation.

This study builds on that contextual foundation to engage with a specific anthropological issue: the identification of trauma in ancient populations. Skeletal trauma is particularly interesting to study because they provide access to lived experiences, risks factors and vulnerabilities of past individuals. Traumas can reflect diverse causes such as accidents, occupational strain, interpersonal violence and on a broader scale, general insecurities of the population. Yet, the analytical potential of trauma remains limited by methodological inconsistences and the lack of a shared diagnostic framework.

As a subfield of bioarcheology, paleopathology, "the science of the diseases which can be demonstrated in human (and animals) remains of ancient times" (Ruffer 1913), has made considerable progress in the classification and description of pathological lesions including

traumas. However, it remains constrained by preservation biases and subjective diagnostic practices. The variability in lesion morphology, challenge the reliability and comparability of trauma analysis. The present study seeks to clarify and propose diagnostic criteria in trauma study by applying a structured, lesion-based approach to a sample of burials and maybe contextualize them.

Broad research problem

The core problem addressed by this study is not merely the documentation of trauma in skeletons, but the epistemological and methodological conditions under which trauma is identified and diagnosed. How can trauma lesions be diagnosed in a consistent and reproductible way? In the face of partial preservation, alterations, what morphological criteria allow for differential diagnosis?

Paleopathological studies often rely on illustrative cases but lack operational precision needed to later construct interpretations(Ortner 2011; Mays 2018). This thesis thus aims to contribute to the refinement of trauma analysis by developing a descriptive and hypothetico-deductive grid, in the hope that it is useful to interpret trauma in others Early Middle Ages necropolis buried, excavated in Île-de-France and even other period and region.

Comparison with clinical diagnostic

In the words of the medical literature, diagnosis by analogy in paleopathology is like what is known as the first-order reasoning system. This system is fast, based on the unconscious, cognitive biases and hypotheses are highly dependent on the experience of the observer. At the same time, a second, slower, conscious, and deliberate system emerges. It is based on analysis and deep reflection on the situation. This system also corrects the errors produced by the first system (Monteiro et al. , 2020) (Charlin et al. 2000)

A concept proposed by B. Charlin and collaborators in 2000, in clinical situations, the practitioners, when confronted with a patient, will search for an appropriate script to diagnose the patient. To restrain his search, he will focus on the information already present in front of him. They will then apply this script to the patient, allowing them to know precisely what information is needed to confirm a diagnosis. When a hypothesis is developed, test is then order, the script allows a reference value and decides whether the results of the test fall within the acceptable range

of the test inside the script and after moving on to the next step of the script. This script is in fact hypothetico-deductive thinking, the second system, and the decision of applying a specific or changing script is based on the first system (Pelaccia et al. , 2011).

In our case, in paleopathology, the corpus of script is lacking. When a lesion is found on dry bones, no script is stored in our knowledge. Furthermore, if a fracture is found, only observation can then confirm a break of the bones. Information can then be missed, depending on what type of fracture or localization on the bones, but those can be useful to determine if the fracture occurred in a specific context (domestic, interpersonal violence etc.) or at least the kinetic need to injure the individuals which is one of the goals of paleopathologic studies. This diagnostic limitation has recently been framed within a dual process model, underlining the absence of established "illness scripts" and the need to combine intuitive and analytical reasoning in paleopathology (Mays 2020).

Definition of core concepts

Trauma is defined as the result of an extrinsic physical force acting upon the body causing a disruption of the tissue (Lovell 1997), this definition refers to etiological[1] origin of the alteration. The International Classification of Disease 11th revision, the definition earlier posed as traumas is closer to the one of injury which is "caused by acute exposure to physical agent, mechanical energy, heat, electricity, chemicals, and ionizing radiations in amount or ate rates exceed the threshold of human tolerance" (WHO, 2025, ICD-11: PA00–PL2Z) thus excluding pathologic traumas resulting of cancerous lytic tumors, for examples.

To ensure a systematic and consistent approach to lesion identification in the skeletal sample, the present work adopts a typological framework based on four elementary bone lesions: abnormal bone formation (ABF), osteolysis, deformity and synostosis (for more illustrations see Appendix 5). These categories were created and defined by me last year and improved this year to encompass both direct and indirect consequences of pathologies and a variety of pathological expressions without immediately linking them into nosological[2] or etiological grid (see Table 1).

[1] of or relating to causes or origins. (https://www.dictionary.com/browse/etiologic)
[2] the systematic classification of diseases (https://www.dictionary.com/browse/nosology)

Elementary Lesions	Definitions	Examples of pathology	Pathological expressions	References
Abnormal Bone Formation	Deposition of new bone in abnormal locations or patterns.	-Traumatic: fracture callus -Infectious: periostitis -Degenerative: arthritis -Neoplastic: bone tumors	Callus formation Marginal osteophytes Hyperostosis frontalis interna	Ortner (2019); Waldron (2009); Morgan et al. (2020)
Osteolysis	Pathological bone loss, erosion, or cavitation due to resorption. Often associated.	-Infectious: osteomyelitis, TB -Traumatic: penetrating injuries -Degenerative: subchondral erosion -Neoplastic: lytic lesions	Gummatous syphilis Osteomyelitic destruction Spinal tuberculosis	Ortner (2019); Waldron (2009)
Deformity	Structural deviation from normal bone morphology or size.	-Post-traumatic: malunion -Metabolic: rickets -Neoplastic: Paget's disease -Genetic: dysplasia	Bowing from rickets Fracture angulation Paget's changes	Waldron (2009); Lovell (1997)
Synostosis	Abnormal or premature fusion between bones, resulting in joint immobility or loss of articulation.	-Post-traumatic: joint fusion -Inflammatory: ankylosis -Congenital: craniosynostosis -Metaplastic: ligament ossification	Ankylosis of joints Spinal fusion Cranial suture fusion	Ortner (2019); Waldron (2009); White et al. (2016)

Table 1 Definitions of the elementary lesion and examples of pathologies and pathological expressions encompass by the elementary lesions (Igor ROLLET, 2025)

The force that is transmitted during the formation of a trauma is the kinetic force. The laws of conservation of energy state that energy cannot be created or destroyed but only changes from one another. During trauma formation, the force resulting of the impact of the body with an object, is absorbed by the body and in some cases is so large that it breaks bony tissues.

Although it could be interesting in studying, perimortem traumas, these lesions require a different approach to build a framework. In a same way, postmortem trauma will not be studied here, it is equivalent in studying taphonomic phenomena. We chose to only study antemortem traumas as they represent the most appropriate categories of traumas for addressing the aims of this study. It is also the one that informs us of the life events of individuals. The diagnostic will be, in part, based on the healing of the trauma.

Fracture repair follows a biological sequence that underlies the diagnostic criteria proposed in this study. After disruption of blood supply and cell death at the fracture site, a fibrocartilaginous matrix forms the internal callus (see Figure 1(b)), while chondrocytes and osteoblasts produce an external callus. Necrotic bones are resorbed and progressively replaced by trabecular bones, later remodeled into compact bones. Each stage (see Figure 1) of this process leaves characteristic morphological correlations, linking the observable criteria on archaeological remains to underlying biological mechanisms (Betts et al. 2022)

Figure 1 Stages in Fracture Repair The healing of a bone fracture follows a series of progressive steps: (a) A fracture hematoma forms. (b) Internal and external calli form. (c) Cartilage of the calli is replaced by trabecular bone. (d) Remodeling occurs. (Betts et al. , 2022)

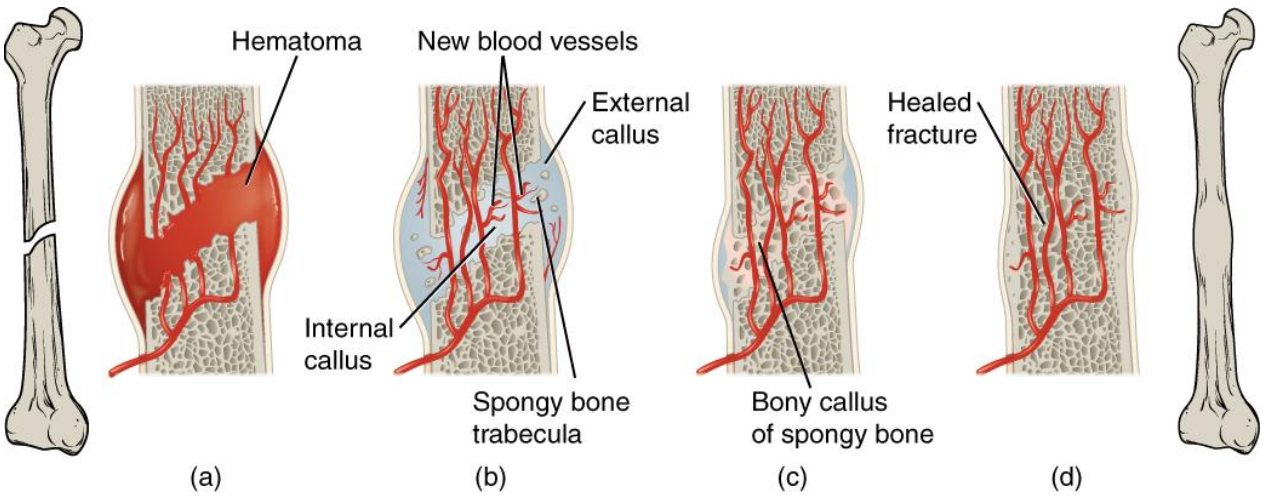

Objectives

In this study, we propose the construction of a reading grid that would not only standardize the description of lesions, but also provide a framework anchored in the context of the sample studied. This approach would make it possible to test the hypotheses formed by the analogical approach. In comparison, the first system would be comparing observed lesions to literature to formulate hypothesis. The reading grid, for traumatic lesions, will be constructed on the sample of anthropological remains from burials acquired during the 1998 and 1972 excavations at Magny-en-Vexin. To build this framework we proposed to standardize the descriptions of the observed lesions to later have a base to discriminate between signs and to organize them in a way that similar signs are closer together and possibly linked to the same diagnosis. Each group would be discriminated against based on the observed lesions but also the other signs observed in the same skeleton. The framework would then differentiate individuals with a singular lesion, different or same lesions diffuse around the skeleton and so on. This study aims to take into consideration the cause of pathology (etiology), mechanical forces.

Material and Methods

Material

The site of Magny-en-Vexin (Val-d'Oise) (see Figure 2 and 3), excavated in 1972 and again during rescue operations in 1997–1998, corresponds to a Merovingian cemetery located beneath the current schoolyard of the Claude Monet secondary school. The 1972 excavation, conducted during the construction of the original school buildings, revealed at least 40 burials, including both stone sarcophagi and inhumations in full-earth pits. However, due to the hurried nature of the intervention, skeletal remains and grave goods were collected in bulk, with limited documentation or stratigraphic control (Sirat, 1972). Consequently, although these findings confirmed the Merovingian character of the necropolis, they are not integrated into the present study's detailed analysis of material culture or burial practices.

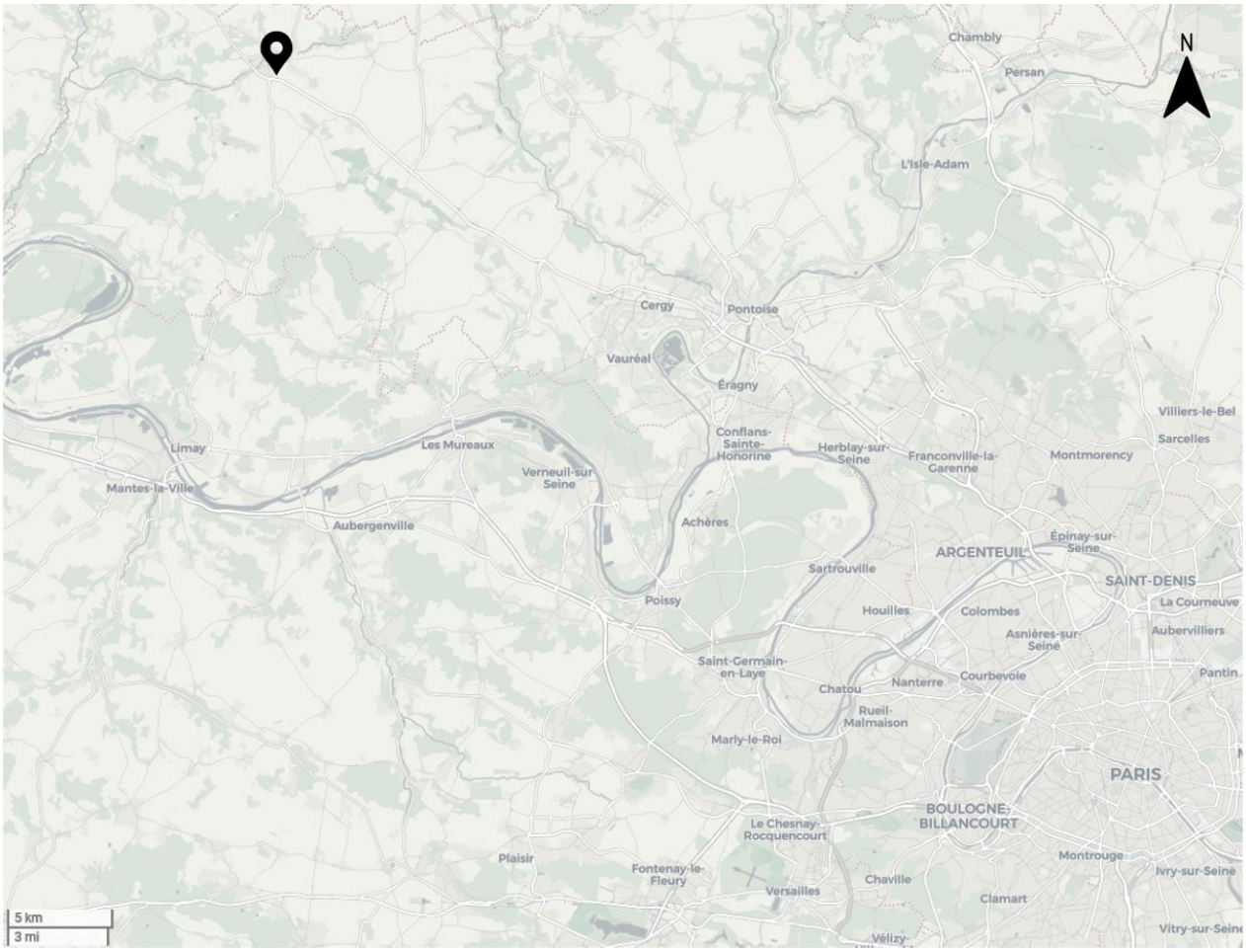

Figure 2 Map of the North-West of the Ile-de-France region, France. Magny-en-Vexin is pinned. © OpenStreetMap France

Figure 3 Map of Magny-en-Vexin, Collège Claude Monet is delimited by the blue polygon. © OpenStreetMap France

The following description is based entirely on the excavation report from 1997-1998 campaign at Magny-en-Vexin (Taupin et al. , 1998) unless otherwise indicated. A total of eleven sarcophagi were discovered, all hewn from local limestone and composed of two quadrangular elements with pitched lids. Coffin presence was inferred in at least ten burials through iron nails, wood traces, or edge-stabilizing stones (e. g. , tombs SEP6, SEP19, SEP22, SEP41, SEP45, SEP59, SEP63), notably concentrated in Sector III (see Figure 4). In other cases, evidence of decomposition in a void suggested burial in a now-decayed wooden container, following the criteria established by Duday (1985). Approximately twenty burials lacked any funerary furniture, including thirteen undisturbed full earth burials, indicating a possible social or chronological distinction.

Grave goods were found in a minority of burials but included diagnostic items such as belt buckles, fibulae, rings, iron knives, beads, and pendants. Tomb S6, for instance, contained a silver ring, a bronze sheet, and an iron knife at the knees. Sector I yielded the highest concentration of prestigious items, including gold and silver jewelry, suggesting the presence of socially distinguished individuals. However, the correlation between richness of grave goods and biological sex or age was not always straightforward, and some richly furnished graves lacked anthropologically confirmed sex attribution.

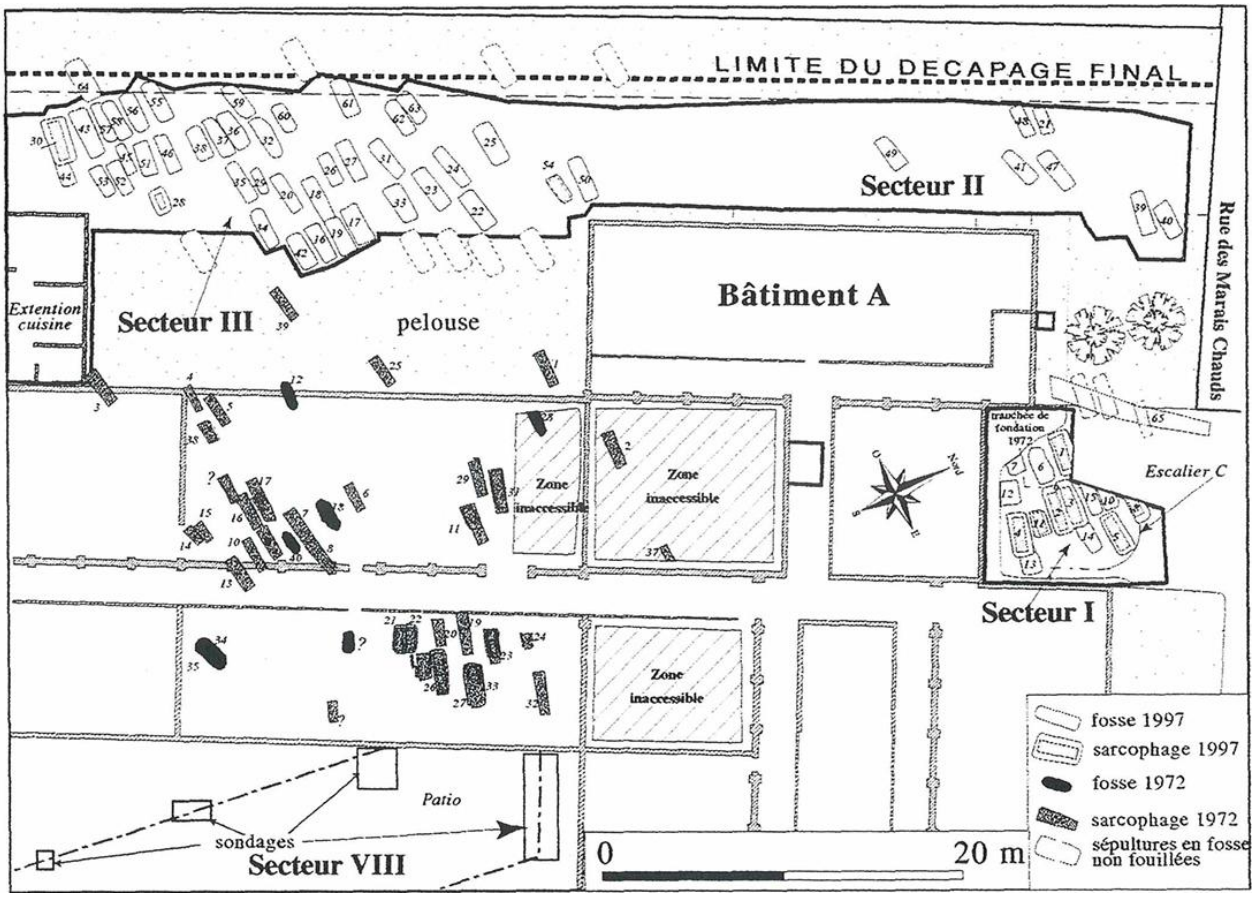

Figure 4 Map of the excavation site of Collège Claude Monet, Magny-en-Vexin, in simple lined and white the fosses excavated in 1997, in full outer line with discontinued inner lined the sarcophaguses excavated in 1997 and in filled black the fosse excavated in 1972, in filled grey the sarcophaguses excavated in 1972 and in discontinued outer line burials not excavated, extracted from the excavation report of the 1998 campaign (Taupin et al. , 1998)

Basic anthropological analyses were conducted on the skeletal remains recovered during the 1997–1998 excavation by C. DUMONT in 1998. Age-at-death estimation was performed using dental eruption stages and long bone development for juveniles, and cranial suture closure for adults (Masset, 1982), revealing a predominance of individuals aged between 18 and 29 years, with very few older than 60. Sex determination was primarily based on pelvic morphology following Bruzek (1991), and cranial features when the pelvis was absent. A total of 17 individuals were identified as male and 16 as female, with some attributions supported by grave goods such as weapons or personal ornaments. The sample of 1997-1998 was used last year by me to test the detection of the elementary lesions.

While these results provide a general demographic outline of the burial population, the methodology reflects the standards of the late 1990s and does not meet current criteria for detailed osteological analysis. No assessments of palaeopathology, activity patterns, or metric data have

been retained in a form suitable for reinterpretation, rendering the dataset obsolete for bioarcheological investigations beyond basic sex and age estimation.

The skeletal preservation varied across the site. Several burials exhibited post-depositional disturbances, including collapse due to sediment compaction and potential looting. Some sarcophagi had been disturbed prior to excavation, complicating the association between grave goods and individuals. Despite this, the combination of funerary architecture, material culture, and anthropological assessment provides a robust foundation for interpreting the burial practices and demographic composition of this Early Middle Ages community.

In total, 62 individuals were sufficiently preserved to be included in the present analysis.

Methods

Conservation

Bone preservation is a critical factor that can impact the detection of pathological lesions. Taphonomic alterations are a major source of pseudo-pathologies, meaning that taphonomic constraints such as plants' root marking the bones can look like a pathology or the destruction of the cortical surface exposing the inner layers of the bones could either be explained by taphonomy or pathology. Thus, we adapt methodologies such as the Anatomical Preservation Index (Bello 2001) (see Table 2) and the Cortical Surface Preservation Index (Dutour 1989) (see Table 3) to assess preservation status. First the conservation is assessed overall skeletal remains linked to one individual but also to specific bones when they present pathological signs using the same criteria: proportion of the bone conserved and preservation of the cortical surface.

Cortical Surface Preservation Index	
Classe 1	Cortical surface completely untainted
Classe 2	More untainted cortical surface than altered cortical surface
Classe 3	As much untainted cortical surface as altered
Classe 4	Less untainted cortical surface than altered cortical surface
Classe 5	Cortical surface fully altered

Table 3 Adaptation of the cortical surface preservation index based on Dutour, 1989

Anatomical preservation Index	
0-25	Estimation in percent of the skeleton preserved
25-50	0% (no preservation)
50-75	100% (the entire skeleton)
75-100	

Table 2 Adaptation of the anatomical surface index based on Bello, 2001

Paleopathological Diagnosis

The diagnostic approach applied to this study followed a two-stage design combining empirical observation with pattern recognition informed by paleopathological literature. The objective is to develop reproducible criteria to assess the traumatic nature of skeletal lesions within the Collège Claude Monet sample.

Initial observation phase: Detection of elementary lesions

During the first year of the research (2024), a systematic macroscopic survey of the osteological remains of the Collège Claude Monet sample from the 1997–1998 excavation was conducted. All preserved anatomical elements were examined under standard lighting conditions using the naked eye or a magnifying glass (10×18 mm) with no enhancement. The aim of this phase was to establish the presence, absence, or non-recordability, and the anatomical distribution of a predefined set of elementary lesions. These included:

- Bone production
- Osteolysis
- Deformation
- Synostosis

These lesions were defined to encompass a substantial proportion of pathological expressions and are based on descriptions in the literature (see Table 1). This phase serves as a primary dataset for later diagnostic work.

This initial phase was intentionally non-interpretive, in accordance with methodological standards that emphasize the necessity of separating observation from diagnosis to reduce confirmation bias (Waldron 2009; Ortner 2019; Mays 2018). Such an approach ensures that the interpretive phase is grounded in reproducible empirical observations.

Pattern recognition phase: Identification of trauma-linked lesions

The second year of research (2025) introduced a pattern recognition strategy designed to isolate lesions potentially attributable to antemortem trauma, and therefore certain categories of elementary lesions. This phase relied on a comparative approach using published paleopathological, clinical, and forensic case descriptions of skeletal trauma as references (Wedel 2013; Judd and Redfern 2011; Ortner 2019; Boyd 2018).

As a first step, individuals presenting with either bone deformation or bone production were identified. These lesions were prioritized because of their frequent association with lesions matching the antemortem fractures described in the literature. Each case was closely examined, and both cases strongly comparable to healed fractures and ambiguous cases were selected for radiographic analysis. The use of pattern recognition grounded in reference literature, primarily Ortner's Identification of Pathological Conditions in Human Skeletal Remains (3rd ed. , 2019), allows for diagnostic interpretation to incorporate both morphological intuition and a comparative framework.

Two cases, the ulnar fracture of SEP 20 and the radial fracture of SEP 33, were positively identified as consistent with classical examples of healed long bone fractures. These individuals exhibited well-defined macroscopic features that matched reference descriptions and were selected as diagnostic standards for the remainder of the study.

Development of diagnostic criteria

Based on the two reference cases identified previously, a set of criteria was developed to distinguish between trauma-related and non-trauma-related lesions. These criteria always start with the morphology of the lesions; they are therefore primarily descriptive. However, unlike general pattern recognition, these criteria focus on precise aspects: the nature of the new tissue, the

characterization of the deformation, and how these features interact. These will serve as positive indicators of trauma.

While the absence of proof is not proof of absence, negative indicators were developed through the observation of lesions that exhibit some characteristics of trauma but do not match the descriptions in the literature and are therefore not necessarily included in pattern recognition. To test the validity and specificity of these criteria, they were applied to other cases in the assemblage exhibiting similar elementary lesions. This allowed for the exclusion of structurally similar but etiologically distinct alterations, reinforcing the diagnostic strength of the selected features.

These steps are designed to address the need for criteria based on lesion features that help guide the paleopathologist toward a diagnosis or a differential.

Integration of ambiguous cases

In the final step, lesions of uncertain origin, those which partially matched trauma-related morphology but lacked definitive features, were assessed individually. These ambiguous cases included:

- Cranial perforations without surrounding remodeling.
- Unilateral synostoses in the absence of contralateral preservation
- Vertebral arch discontinuities lacking reactive bone.

Each case was evaluated using the diagnostic framework as a base, but specific criteria were added depending on the bone or the injury in question. Radiographic criteria were also incorporated and proved essential.

Ultimately, it became necessary to add new criteria to accommodate a wider range of trauma presentations described in the literature. High-velocity trauma, fractures of flat bones, or vertebral injuries may appear morphologically different from the reference cases selected.

Medical imaging, including X-ray and CT scanning, was used in selected cases to evaluate bone structure and density. Radiographic images were digitally processed by adjusting exposure and brightness or inverting colors to enhance visibility of internal structures, such as the medullary cavity, trabecular tissue, or diploe.

The use of a hypothetico-deductive structure was essential in addressing the complexity of ambiguous lesions. As Judd (2008) and Ortner (2019) underline, morphological uncertainty

requires the careful balancing of empirical pattern recognition with a contextualized understanding of skeletal response to injury.

In doing so, the methodology moved beyond isolated morphological description and toward a reproducible, evidence-based framework for identifying trauma in archaeological skeletal populations.

Construction of Kinetic Syndromes.

Kinetic trauma syndromes refer to recurring and interpretable patterns of skeletal injury that correlate lesion distribution and severity with inferred biomechanical forces. Based on current clinical data, the goal is to construct a comparative model that allows us to hypothesize the energy level and mechanism of trauma of the bone tissue, without necessarily assigning a definitive cause.

The model operates under the assumption that skeletal injuries can be classified according to the level of kinetic energy involved in their production. For this study, three broad energy categories will be defined:

- Low-energy trauma: typically resulting from incidents such as falls from standing height, where the impact is mild and the energy transferred to the skeleton is slightly exceeding the physiological threshold required to cause skeletal trauma.
- Medium-energy trauma: associated with events such as blunt force impacts, minor vehicular accidents, or falls from moderate heights, where the energy transferred to the body clearly exceeds the physiological trauma threshold.
- High-energy trauma: resulting from events involving significant force, such as falls from great heights, crush injuries, or high-speed impacts, where the energy transmitted to the body significantly exceeds the physiological threshold required to cause skeletal trauma.

To construct this model, a targeted review of biomedical and clinical literature was conducted. The selection focused on large-scale epidemiological studies involving several thousand individuals, ensuring a robust statistical basis for inferring generalizable patterns. Articles narrowly focused on highly specific anatomical regions or rare injury types, such as isolated femoral neck fractures, were excluded to avoid overrepresentation of specialized clinical contexts.

The study by Almigdad et al. (2022), based on over 3000 hospitalized trauma patients, demonstrates that the energy of trauma is the principal determinant of fracture distribution and severity, irrespective of patient age or sex. It also highlights consistent patterns across anatomical

regions, with high-energy mechanisms such as road traffic accidents and falls from height producing frequent fractures in the pelvis, spine, long bone shafts, and scapula, whereas low-energy events, especially among elderly females, more commonly affect the proximal femur, thoracic spine, and distal humerus. These patterns are essential in guiding the structuring of kinetic trauma categories for archaeological interpretation.

The literature reviews prioritized studies that report injury distributions across broad anatomical regions frequently involved in both accidental and intentional trauma. These include:

- Cranial vault and facial bones
- Vertebral column
- Upper limb: humerus, radius, and ulna
- Lower limb: femur, tibia, and fibula
- Lower extremity: tarsal and metatarsal bones

The results of this review will inform the construction of trauma energy categories to be applied to the lesion profiles observed in the Magny-en-Vexin skeletal sample.

Results

Conservation

Conservation was also studied, in mature and immature individuals, using the Anatomical Conservation Index (ACI) and the Cortical Surface Conservation Index (CSCI). The classes showing the least conservation are in the majority across individuals. The class showing no conservation of the cortical surface (Class 5) comprises 32 individuals meaning (see Figures 7 and 8) 50.8%, while the class with a cortical surface greater than the healthy cortical surface (Class 4) comprises 30 individuals meaning 49.2%. For ACI, the lower category (0-25%) represents 47.5% and the upper category (75-100%) represent 26,2% while each middle categories represent 13.1% (see Figures 5 and 6).

Overall, the results of the conservation study indicate both poor skeletal preservation and poor cortical conservation.

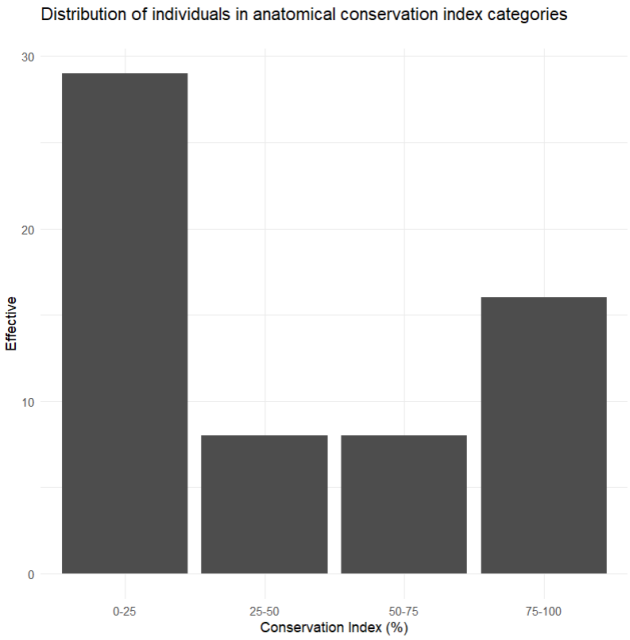

Figure 6 Diagram of the numbers in relation to the anatomical conservation index of each burial, Collège Claude Monet, Magny-en-Vexin (excavation of 1997-1998). ROLLET, 2024

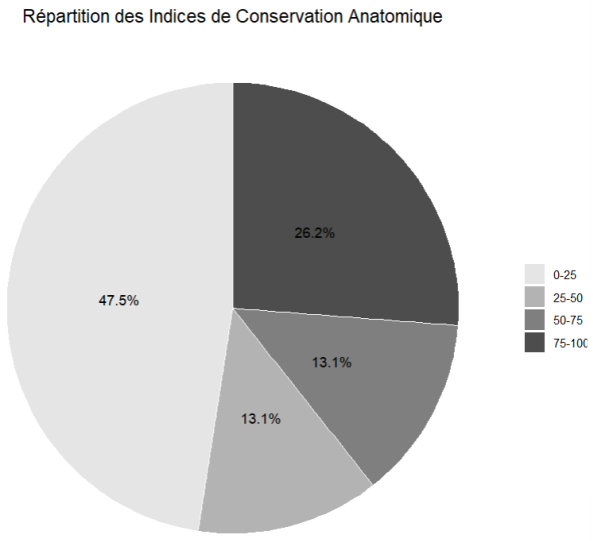

Figure 5 Distribution of burials by anatomical conservation index categories, Collège Claude Monet, Magny-en-Vexin, excavation of 1997-1998. ROLLET, 2024

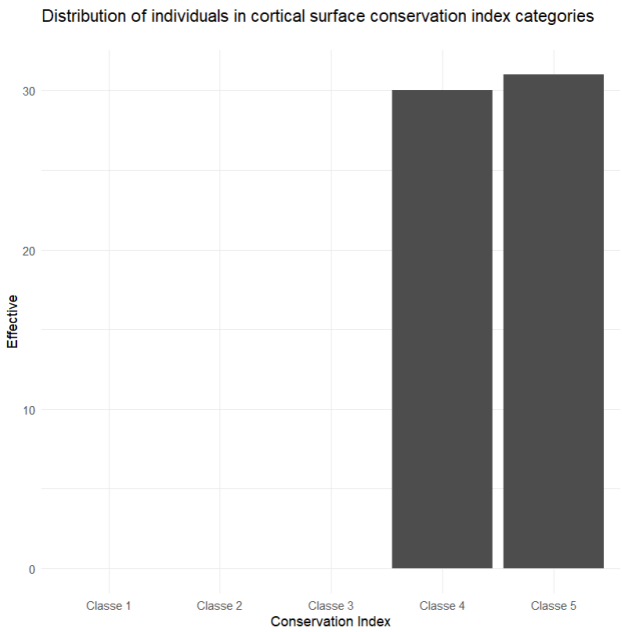

Figure 8 Diagram of the numbers in relation to the conservation index of the cortical surface of each burial, Collège Claude Monet, Magny-en-Vexin (excavation of 1997-1998). ROLLET, 2024

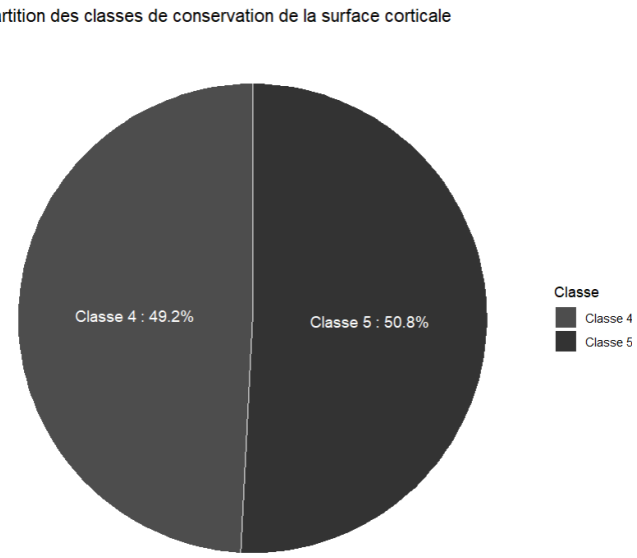

Figure 7 Distribution of burials by cortical surface conservation index categories, Collège Claude Monet, Magny-en-Vexin, excavation of 1997-1998. ROLLET, 2024

Paleopathological Diagnosis

Detection of elementary lesions

Last year, 2024, the presence or absence of elementary lesions was tested on every individual. The presence and localization or absences of the lesions were recorded for each individual. Based on 65 bone assemblages, with individuals grouped by burial for the 1998 excavation and by anatomical region for the 1972 material. Out of the 61 individuals, 21. 5% (n= 13) shows at least one elementary lesion, 18% (n=12) shows at least one bone production, 9% (n=6) shows at least one osteolysis, 12% (n=8) shows at least one deformation and 3% (n=2) shows one synostosis (see Table 4).

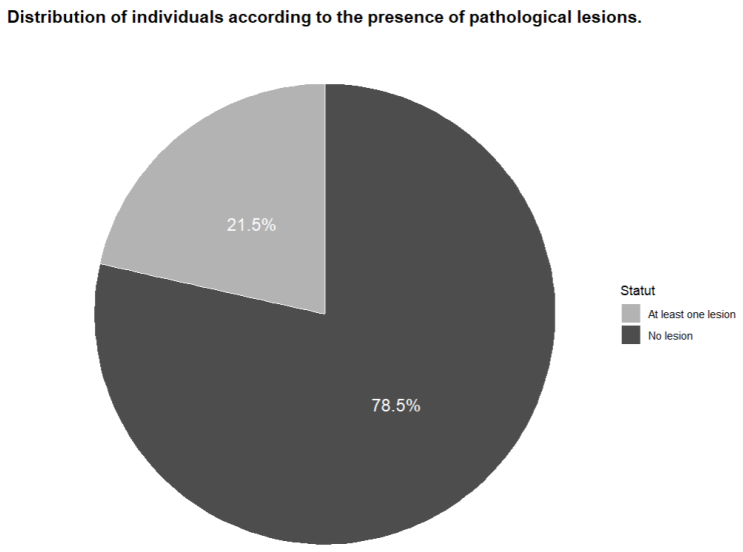

Figure 9 Distribution of individuals according to the presence or absence of pathological elementary lesions.(ROLLET, 2024)

Table 4 Summary of presence or absence (0) of elementary lesions (bone production, osteolysis, synostosis, deformation) among individuals presenting at least one lesion. For each lesion recorded as present, anatomical location is specified. (Tx = thoracic vertebrae; Lx = lumbar vertebrae; R = right; L= left)

Burial ID (Year, type, N°)	Bone production	Osteolysis	Synostosis	Deformation
72 no US (E 14 à19)	Rachis + Radius	0	0	0
97 SEP 13	0	Frontal R	0	0
97 SEP 2	Rachis (1Tx+3Lx)	0	0	0
97 SEP 20	0	0	0	Ulna L
97 SEP 21 LOT 1	Skull (Frontal + Parietal)	0	0	Parietals L&R
97 SEP 23	0	0	Sacroiliac	Tibia L
97 SEP 25	Rachis (C2+3Tx)	Rachis (C2+3Tx)	0	0
97 SEP 27	0	Rachis (C2+2Tx) + 1 Rib	0	Skull (Occipital + Parietal)
97 SEP 3 US 21 LOT 1 + SEP 3 US 8 LOT 1	Rachis (1Tx + 3Lx)	Radius L + MT3 R + Rachis (Lx)	0	Rachis (2Lx)
97 SEP 33	Fibula R + Scapula L + Radius R	Parietal L	0	Tibia R + Calcaneus L + Talus L
97 SEP 44	Frontal L	Frontal L	0	0
97 SEP 59 US 196	0	0	0	R Lower Limb
97 SEP 8	Rachis (Lx)	0	0	Parietal L
97SEP 42	Cuneiform L + Rachis (Lx)	0	Calcaneus R + Navicular R	Talus R

Pattern recognition

Pattern recognition allows the recognition traumatic signs on the sample from the burials of Magny-en-Vexin. The first phase of the deep analysis consists of identifying elementary lesions and evaluating their diagnostic orientation regarding trauma. The assessments of lesion patterns rely on macroscopic observations in accordance with the definition given (see Table 1)

Positives elementary lesions: Deformation and Bone productions

Figure 10 Posterior overview of the left ulna from SEP 20, showing bone curvature and surface thickening. Collège Claude Monet, Magny-en-Vexin, excavation of 1998. (Ant. = Anterior, Dist. = Distal).

In our sample, deformation is the most consistent indicator of healed bone trauma particularly when it involves angular changes or displacement in long bones (see Figure 10). When deformation is observed in association of contact bone production the orientation toward antemortem trauma is stronger. The diagnostic contribution to bone production is only positive when it is focal and associated with shape abnormality. As for deformation, diffuse, bilateral, or symmetric bone production may suggest systemic pathology, such as scurvy, osteomyelitis, or fluorosis (Ortner 2019) thus excluding the trauma etiology.

Cited pathologies as counterexample of the positive aspect of deformation and bone production exhibit another elementary lesion.

Negative elementary lesions: Osteolysis

Osteolytic lesions can be considered indicative of trauma only under specific conditions. In this sample, osteolysis was interpreted as potentially traumatic when it appeared as a macroscopic isolated lesion (see Figure 11 and Figure 12) , regardless of bone type or anatomical location.

However, a critical interpretive limitation arises when such lesions are located on articular surfaces, where non-traumatic causes, particularly degenerative or infectious processes, are far more likely.

Traumatic osteolysis is typically non-specific in pattern, involving cortical and subcortical bone without regard for underlying structural logic. In contrast, osteolysis linked to pathological conditions often preserves the architecture of the affected region and aligns with known disease mechanisms.

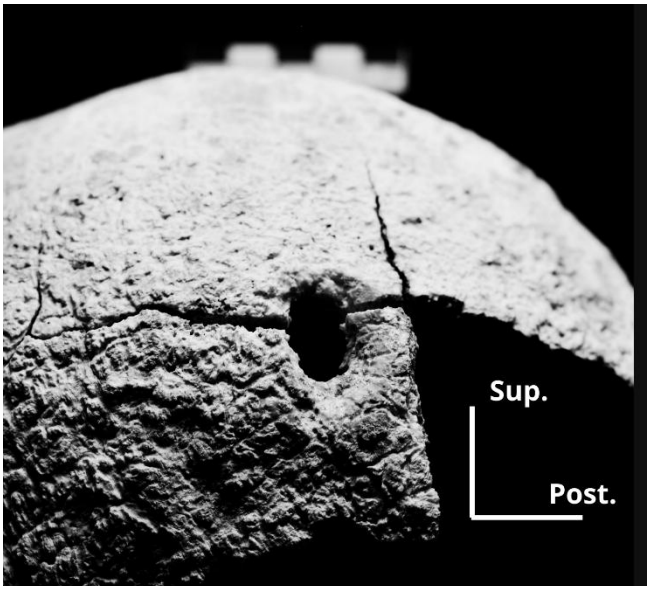

Figure 11 Lateral external view of the skull from SEP 33, with a circular depression on the left parietal region. Collège Claude Monet, Magny-en-Vexin, excavation of 1998. (Sup. = Superior, Post. = Posterior).

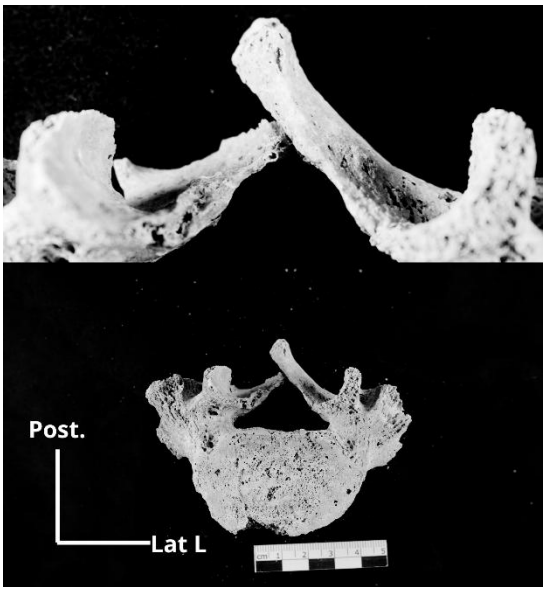

Figure 12 Superior view of adjacent lumbar vertebrae from SEP 3 US8 LOT 1, including overview and detail of spinous processes. Discontinuity of the neural arch is visible. Collège Claude Monet, Magny-en-Vexin, excavation of 1998. (Post. = Posterior, Lat. L = Lateral Left).

Moreover, in cases of trauma, osteolysis is frequently accompanied by bone apposition a reparative response. In these scenarios, newly formed bone appears in direct continuity with the lytic zone, forming a unified lesion complex. This stands in contrast to degenerative processes, where new bone formation, like osteophytes, typically occurs in the same anatomical region but remains spatially distinct from the lytic areas.

Undefined contribution: Synostosis

Synostosis, the bony fusion of adjacent skeletal elements, represents a challenge in the recognition of traumatic patterns. While antemortem trauma is an accepted cause of fusion it is equally accepted as the results of congenital or of chronic biomechanical stress[3]. Examples include sacroiliac fusion that can be observed in case of ankylosing spondylitis, for SEP 23 and clacaneonavicular synostosis of SEP 42 (see Figure 13). In traumatology, synostosis is cautiously considered when it appears unilaterally, without matching counterparts on the contralateral side.

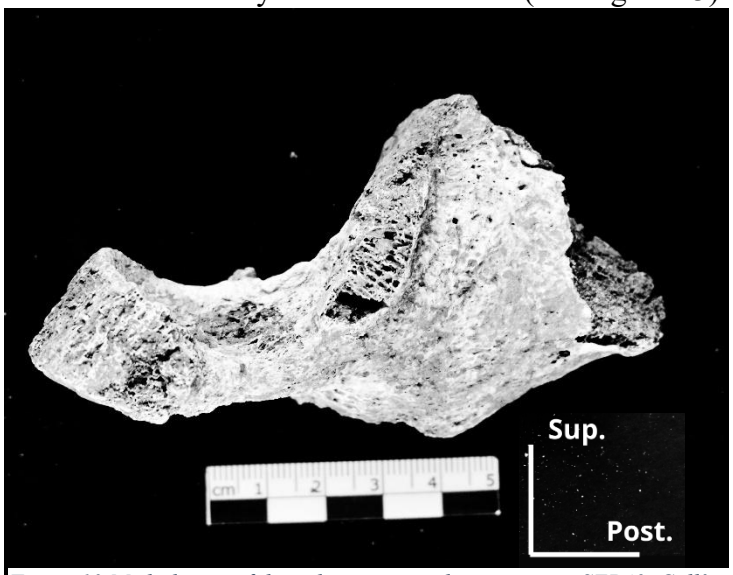

Figure 13 Medial view of the calcaneonavicular synostosis SEP42, Collège Claude Monet, Magny-en-Vexin, Excavation of 1997-1998. (Sup= Superior; Post. = Posterior).

However, the primary distinction must first rely on the elementary lesion itself. A fracture is, by definition, a discontinuity of the cortical surface, whereas a synostosis represents an abnormal healing response leading to osseous bridging. Only once this biological distinction is established should additional features, such as contralateral preservation or symmetry, be considered to refine interpretation. In this study, the synostoses were observed in individuals where the opposite side could not be reliably assessed due to preservation, but the initial evaluation must remain anchored in the recognition of cortical discontinuity versus abnormal fusion.

Synthesis and borderline cases

Macroscopic analysis of the sample revealed that certain elementary lesions are more likely to support a diagnosis of trauma than others. The combination of localized deformation and bone production consistently appeared among the strongest indicators. This association reflects the underlying biomechanical and biological processes: a sudden external force produces a cortical discontinuity and angular deviation, while the subsequent reparative response generates focal callus

[3] Biomechanical stresses can be described as micro-traumas (Myklebust et al. 1988) but is not an injury caused by sudden high intensity rise of forces which is the definition chosen in this study (see Definition of core concepts)

deposition at the fracture margins. Together, these features are therefore direct signatures of both the traumatic event and the healing process. In contrast, osteolysis, particularly when confined to articular surfaces, is more often the result of degenerative or infectious mechanisms. Its morphological presentation, such as cavitations with preserved architecture or peripheral sclerosis, does not correspond to the sequence of bone repair after trauma, and it thus functions as a negative indicator. Synostosis, while notable, is best considered diagnostically neutral. Although it can occasionally follow joint injury, more commonly it represents congenital fusion or long-term biomechanical stress, and the frequent absence of reactive remodeling further weakens its value as an isolated marker of trauma.

Positives cases corresponding to the description of the presentation of fracture in the literature have been identified the radial fracture of SEP 33 and the ulnar fracture of SEP 20. Comparing the lesions to the description made (Wedel, 2013; Waldron, 2009; Ortner, 2019).

Several borderline cases illustrate the limitations of relying solely on pattern recognition. For example, sacroiliac and calcaneonavicular fusions present as synostoses without any accompanying bone reaction or remodeling. These cases do not show associated trauma elsewhere in the skeleton, which prevents any confident attribution to injury. Other ambiguous examples include a deformed calcaneus (see Figure 14, and Figure 15), a cranial perforation (SEP 33), and vertebral foramen ruptures in SEP 56 and SEP 3 US8 LOT 1. These lesions are limited to cortical discontinuities or isolated structural changes, without signs of repair or inflammation. Such cases highlight the diagnostic uncertainty that arises when lesions do not conform to expected patterns of trauma or healing.

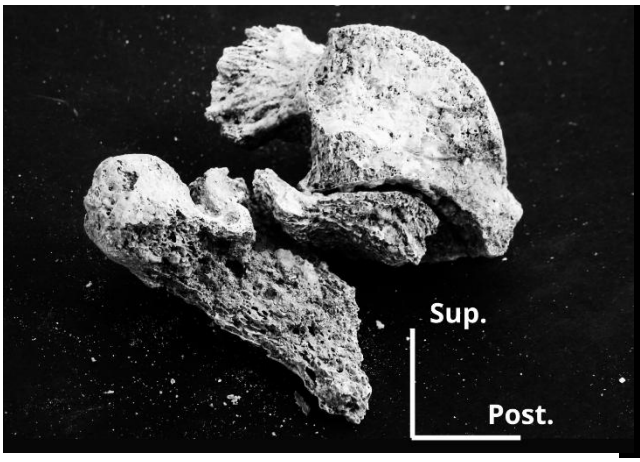

Figure 14 Overview of the talo-calcaneal joint in SEP 33 (left), with sagittal medial and superior views (right) showing marked angular deformation of the calcaneus. Collège Claude Monet, Magny-en-Vexin, excavation of 1998. (Sup. = Superior, Med. = Medial).

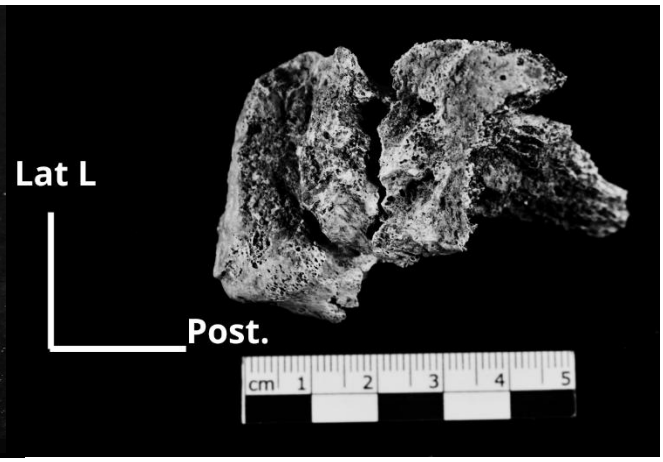

Figure 15Posterior close-up of the lesion on the left ulna of SEP 20, illustrating cortical thickening. Collège Claude Monet, Magny-en-Vexin, excavation of 1998. (Prox. = Proximal, Med. = Medial).

Taken together, these observations underscore the need for a structured, hypothetico-deductive framework. Rather than relying on visual resemblance or isolated morphological features, diagnosis must be supported by reproducible reasoning and criteria that can account for both clear and ambiguous cases. The definition and application of these criteria will be addressed in the following section and are based on certain lesions in the sample, the ulnar fracture of SEP 20 and the radial fracture of SEP 33.

Proposed criteria to support the fracture diagnosis

Based on macroscopic observations of fully positive pattern recognition traumatic lesions

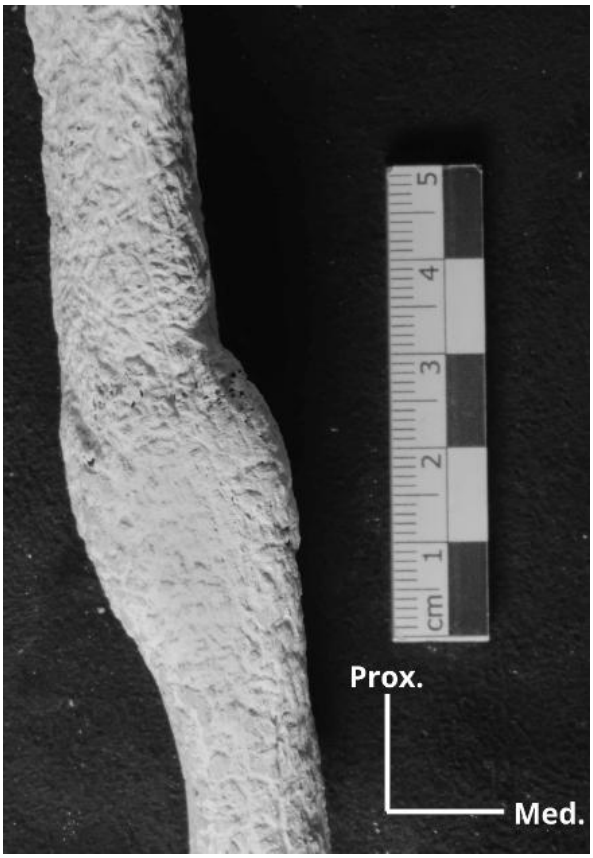

Figure 17 Posterior close-up of the lesion on the left ulna of SEP 20, illustrating cortical thickening. Collège Claude Monet, Magny-en-Vexin, excavation of 1998. (Prox. = Proximal, Med. = Medial).

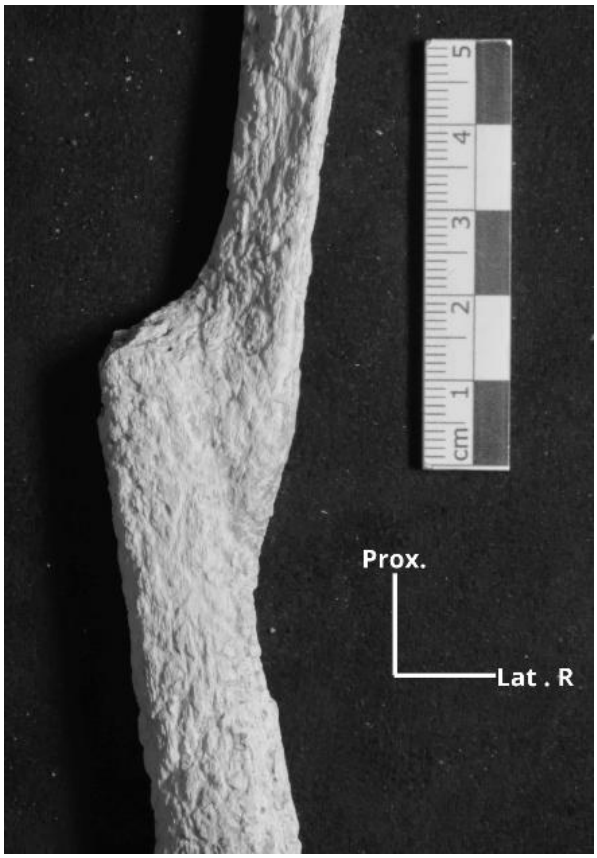

Figure 16 Frontal close-up of the right radius lesion from SEP 33, with overlapping of anatomical landmarks. Collège Claude Monet, Magny-en-Vexin, excavation of 1998. (Prox. = Proximal, Lat. R = Lateral Right).

Upon observation of the ulnar lesions of SEP 20 (see Figure 17) and radial lesions of SEP 33 (see Figure 16), we can observe that the deformation is harsh and localized, pre fragment and post fragments show no signs of other alterations (apart from taphonomy), the bone production is in direct contact with the site of deformation, localized it shows no discontinuity, no macroscopically visible cavity or perforation. Apart from taphonomic alterations, the bone remodeling is smooth, has no regard for anatomical landmarks (such as insertion) and is in superposition compared to the level of the fragment . The presence of the criteria was recorded (see Table 5).

Table 5 Presence (+) or absence (-) of macroscopic morphological features observed on SEP 20 (ulna) and SEP 33 (radius)

Elementary lesions concerned	Proposed criteria	Presence on sample	
		Ulna SEP 20	Radius SEP 33
Deformation	Localized	+	+
	Abrupt linear	+	+
	Fragment displacement	+	+
Bone production	Direct and full contact	+	+
	Limited on the deformation	+	+
	Smooth	+	+
	Cavity and/or porosity	-	-
	Masking anatomical landmarks	+	+
	Overlapping edges	+	-

Based on X-ray imaging of fully positive pattern recognition trauma lesions

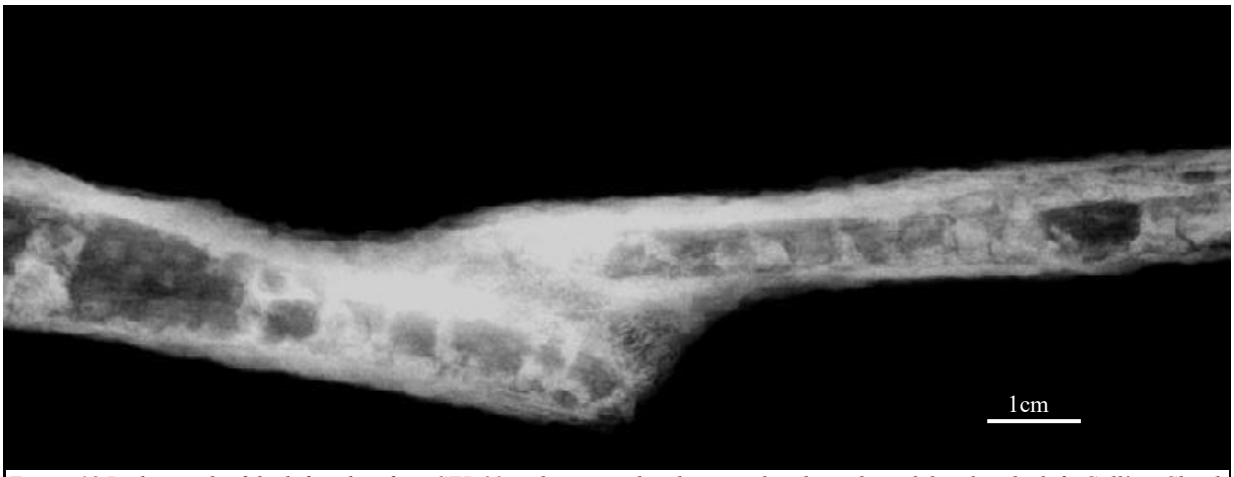

Figure 18 Radiograph of the left radius from SEP 33 with proximal end oriented to the right and distal to the left. Collège Claude Monet, Magny-en-Vexin, excavation of 1998.

Standard X-ray imaging allows for the visualization of internal structures of the bone and the lesion. On the radial lesions the imaging were conclusive (see Figure 18, also see radiography of the ulna, Appendix 4). The lesion believed to be antemortem fracture shows a bone remodeling as dense as the cortical bone, recovering the medullar cavity linking only the two fragment without invading the medullar cavity. Both fragments show no loss in parallelism. The presence of the proposed criteria was recorded (see Table 6).

Table 6 Radiographic criteria documented in SEP 20 and SEP 33 (+ = presence)

Elementary lesions concerned	Proposed criteria	Presence on sample	
		Ulna SEP 20	Radius SEP 33
Deformation	Fragment conserved cortical integrity	+	+
	Cortical parallelism at rupture site	+	+
	Cortical discontinued	+	+
Bone production	Unifies fragments	+	+
	Covers the entire exposed medulla	+	+
	Exterior density equal to cortical bone	+	+
	Spongy in the center	+	+
	No medullary invasion observed	+	+

Integration of ambiguous cases: Macroscopic observations

Observation of the cranial vault of SEP 33 reveals a localized funnel shaped defect penetrating inside the skull. The rounded edges masking the diploe. On the intern table, a limited zone of thickening is observed around the defect. No bone displacement or angularity is observed, and the lesion is unique and isolated. An adjacent fissure, presenting no remodeling, serves as an internal control, emphasizing the distinction between taphonomic cracks and biologically active lesions. On the same burial, the space between the facet for the cuboid and the posterior talar facets shows a harsh angular deformity with no signs of bone production. The other bones of the tarsi show no other signs.

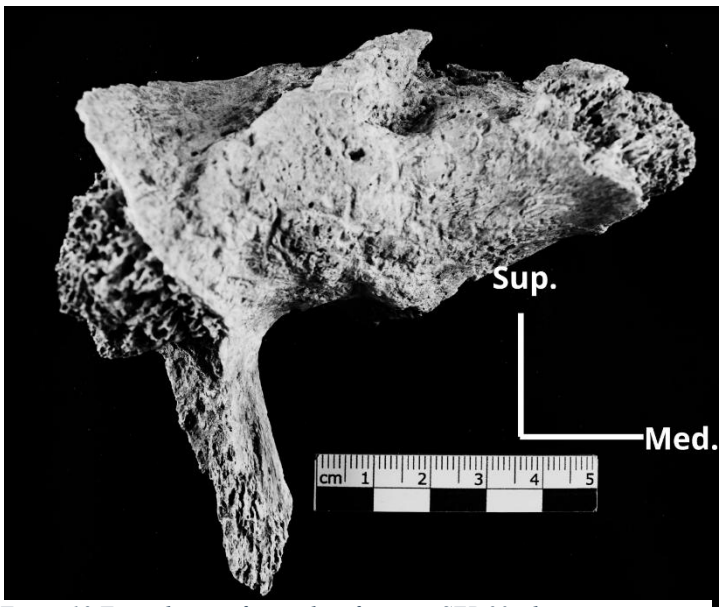

Figure 19 Frontal view of sacroiliac fusion in SEP 23, showing continuous ossification between the ilium and sacrum. Collège Claude Monet, Magny-en-Vexin, excavation of 1998. (Sup. = Superior, Med. = Medial).

For synostosis cases, the sacroiliac fusion is exhibited as a bony bridge between the auricular surface of the iliac bone and the sacrum (see Figure 19). The bridge is a continuous sheet disregarding the normal joint boundaries. The lack of bilateral preservation prevents assessment of symmetry but the literature overview confirmed as being a criterion for trauma diagnosis (Ortner, 2019; Waldron, 2009). A similar argument can be made for the second synostosis observed in the sample. The clacaneonavicular fusion shows no sign of bone production. However, the bridge shows an adaptation to the talar articulation.

Integration of ambiguous spinal cases: Macroscopic observations

Figure 20 Posterior view of a lumbar vertebral body from SEP 3 US8 LOT 1, showing transverse asymmetry and disrupted vertical alignment. Collège Claude Monet, Magny-en-Vexin, excavation of 1998. (Sup. = Superior, Lat. R = Lateral Right).

Because of the various aspects given to trauma on the vertebral bodies, ambiguous cases need to be treated separately.

A lumbar vertebral body (SEP 3 US 8 LOT 1) shows a progressive narrowing from right to left (see Figure 20). This loss of parallelism conflicts with proposed criteria for fracture. This transverse thinning appears uniform and continuous, without surface fragmentation or cortical bridges (apart from taphonomic alterations), Neighboring vertebrae exhibit the same patterns of deformation. In the sample, two vertebral arches are incomplete, on the same individuals as the deformation of the vertebral body, a clear fracture (as in a break in the bone not as a diagnosis) of the neural arch is observed near the spinous process on

the right side. Another individual exhibits a complete and bilateral fracture of the neural arch, isolating it from the vertebral body and the mamillary process. No signs of bone production are observed. Taking together the deformation and break on SEP 3 US 8 LOT 1 are linked to compression forces and thus corresponding to the definition of trauma (Ortner, 2019).

Integration of ambiguous cases: X-ray imaging

Regarding the skull of SEP 33, radiographic imaging revealed not only a localized thickening of the internal table (see Figure 22, for complete image see Appendix 4) and sealing of the diploe, but also a cortical fragment still attached to the inferior margin of the defect. This feature is consistent with a depressed fracture (in French "embarrure"), characterized by an inward displacement of a bone fragment at the site of impact. (see Figure 21, for complete image see Appendix 4) The associated remodeling, including cortical thickening and trabecular closure, further supports the interpretation of this lesion as a healed depressed fracture rather than a non-traumatic defect.

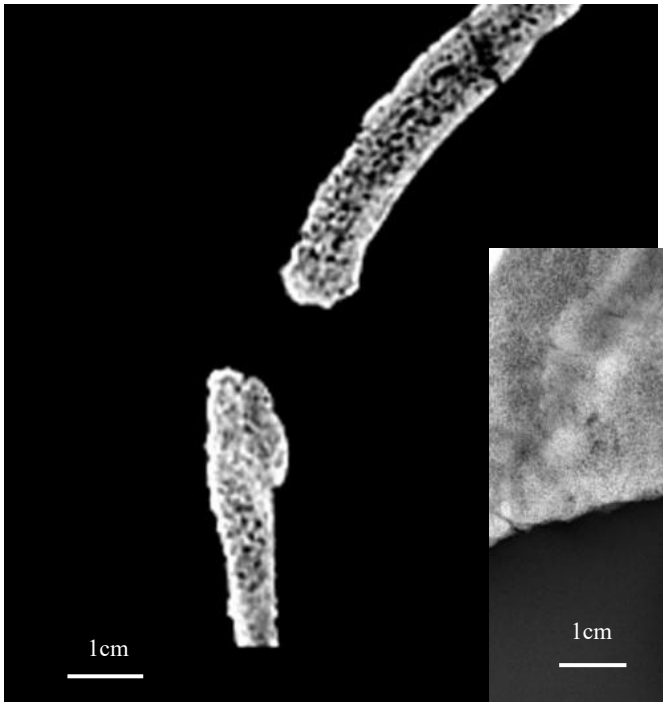

Figure 21 Sagittal CT slice of the skull from SEP 33 (position: L = 562; W = 1873), showing a funnel-shaped lesion and local thickening of the internal table. Collège Claude Monet, Magny-en-Vexin, excavation of 1998.

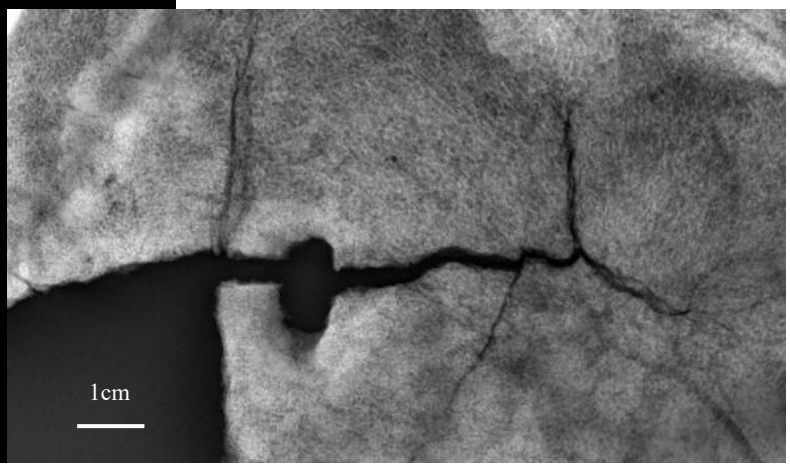

Figure 22 Lateral radiograph from the inside of the skull from SEP 33, zoomed on the lesion. The denser remodeling is visible as increased radiographic brightness. Collège Claude Monet, Magny-en-Vexin, excavation of 1998

In the same individuals, the X-ray of the left calcaneus exhibits no other signs that could not be explained by taphonomy (see Appendix 4), the variation in density is concurring with the presence or absence of bone. Still the deformation is concerning because of its harshness.

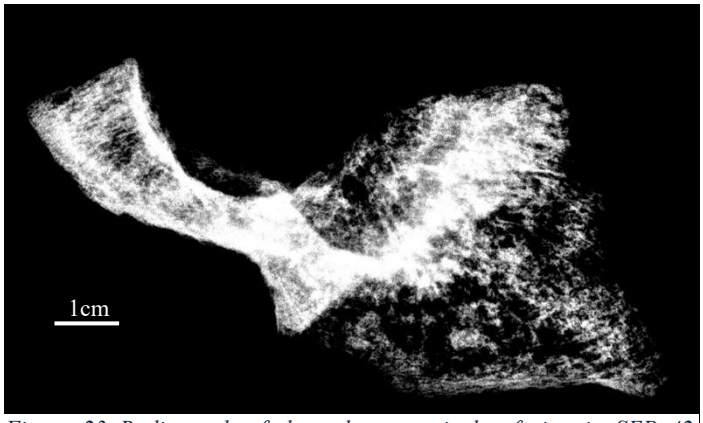

Figure 23 Radiograph of the calcaneonavicular fusion in SEP 42. Density differences are considered likely due to taphonomic alterations. Collège Claude Monet, Magny-en-Vexin, excavation of 1998.

Regarding synostosis, the clacaneonavicular fusion shows no other signs on the x-ray, no anomaly of density is observed, despite taphonomic bone loss, the fusion has a constant density (see Figure 23, for another view see Appendix 4). The imaging of the sacroiliac fusion of SEP 23 was inconclusive, although at the lowest setting there are not enough details to have correct reading.

Synthesis: The proposed criteria for bone fracture

When the presence or absence of the criteria is tested in ambiguous cases (see Table 7), a decision can be made with a certain level of certainty. While the reference of trauma (Ulna SEP 20 and Radius SEP 33) accumulates a lot of criteria, new criteria based on the ambiguous cases and literature review it emphasize that specific presentation of trauma can remain undetected (Vertebrae SEP 56). The grid then only shows that the Skull of SEP 33 is in fact a trauma. While it is not a long bone fracture but a perforation of the skull, a certain similarity in terms of criteria was observed and more criteria reenforcing the diagnostic were developed.

Table 7 Comparative synthesis of macroscopic and radiographic observations for SEP 20, SEP 33, SEP 3 US8 LOT 1, SEP 42, and SEP 23. (+ = presence: - = absence).

Elementary Lesions	Criteria	Reference (Ulna L SEP 20 + Radius R SEP 33)	Skull SEP 33	Calcaneus L SEP 33	Vertebrae Lx SEP 56	Sacroiliac R SEP 23	Clacaneonavicular R SEP 42
Macroscopic Deformation	Localized	+	+	+	-	-	-
	Abrupt linear	+	+	+	-	-	-
	Fragment displacement	+	-	-	-	-	-
Macroscopic Bone production	Direct and full contact	+	+	-	-	-	-
	Limited on the	+	+	-	-	-	-
	Smooth	+	+	-	-	-	-
	Cavity and/or porosity	-	-	-	-	-	-
	Masking anatomical landmarks	+	+	-	-	-	-
	Overlapping edges	+	+	-	-	-	-
Macroscopic osteolysis	Funnel-shaped defect	-	+	-	-	-	-
	Thickened internal table	-	+	-	-	-	-
	Smooth internal margin	-	+	-	-	-	-
	Isolation of lesion	-	+	-	-	-	-
	Absence of outer table breach	-	+	-	-	-	-
X-ray Deformation	Fragment conserved cortical integrity	+	-	-	-	-	-
	Cortical parallelism at rupture site	+	+	+	-	-	-
	Cortical discontinued	+	+	-	-	-	-
X-ray Bone production	Unifies fragments	+	-	-	-	-	-
	Covers the entire exposed medulla	+	+	-	-	-	-
	Exterior density equal to cortical bone	+	+	-	-	-	-
	Trabecular-like in the center	+	+	-	-	-	-
	No medullary invasion observed	+	+	-	-	-	-

Interpretation of the criteria

If the proposed criteria are simple in their description, they are linked to healing process or physical presentations. An abrupt, linear deformation without curvature indicates a sharp, angular break typically resulting from trauma, in contrast to gradual plastic deformation (Lovell, 1997; Waldron, 2009). Similarly, a localized deformation suggests a mechanical injury rather than a systemic condition such as rickets (Ortner, 2019; Lovell, 1997). A clear break in the cortical bone, known as cortical discontinuity, is a key indicator of a fracture and confirms its traumatic origin (Roberts & Manchester, 2010). Fragment displacement and overlapping edges point to a complete fracture without post-traumatic repositioning and may indicate compressive forces leading to misaligned healing (Ortner 2019; Aufderheide and Rodríguez Martín 2011; Lovell 1997).

Radiographically, the preservation of cortical integrity in fracture fragments, without distortion, suggests an acute break with no plastic deformation (Ortner, 2019; Lovell, 1997). The presence of bone bridging between fragments confirms an antemortem origin and reflects the initiation of physiological repair (Ortner, 2019; Aufderheide & Rodríguez-Martín, 2011). The complete endosteal sealing of the exposed medullary cavity, along with peripheral bone exhibiting the same density as the original cortex, indicates advanced consolidation and the final stage of remodeling (Waldron, 2009; Ortner, 2019; Lovell, 1997). Trabecular regeneration in the middle portion of the bone also demonstrates structural restoration (Martinez-Zelaya et al. 2021). Moreover, the absence of abnormal medullary invasion rules out infection or aggressive pathological processes, while excessive bone production that obscures normal anatomical landmarks points to unstable or misaligned healing (Ortner, 2019; Waldron, 2009).

Finally, smooth bone formation confined to the site of injury, without evidence of cavitation or porosity, suggests an organized, non-infectious healing response. This excludes chronic inflammatory or metabolic conditions such as osteomyelitis (Ortner 2019; Waldron 2009; Roberts and Manchester 2010; Lovell 1997). Together, these macroscopic and radiographic criteria provide a comprehensive framework for distinguishing a well-healed antemortem fracture from non-traumatic bone diseases.

Kinetic syndromes

The overview of the literature of fracture epidemiology with frequency and etiologic mechanisms allows a categorization of the different anatomical regions in different kinetic syndromes. Derived from high sample studies, primarily based on recent data collection from the emergency departments. Each bone or anatomical region is described with frequencies of fracture, the size of the sample and the etiological mechanism. The data was restrained to adults only. Overall, this data will allow us to formulate hypothesis of the violence of the trauma, a step closer toward etiology. The more fatal it is, the less frequent and linked to high energy mechanisms such as Motor Vehicle Accident (MVAs) the more likely they are the result of a high kinetic energy event.

Based on the nature of the mechanisms observed to lead to a fracture, the anatomical region and bones are divided into three categories: high, medium and low. The classification (see Table 8), is not intended to capture the total complexity of trauma but rather operationalize general patterns that are consistent at least of modern generation but multiple studies.

Table 8 Overview of the epidemiological data, organized by anatomical region and bone in cranio-caudal order, with incidence, frequency; sample size, population of the study; etiologic mechanisms; references of the studies. In red relating to high energy, orange to medium energy and Yellow to low energy,

Bone Region	Incidence / Frequency	Sample Size / Population	Etiological Mechanisms (main)	References
Cranial Vault	Vault fractures: 88.4% (fatal), 75.3% (non-fatal)	n=1,260 isolated head trauma (Turkey)	High-energy blunt trauma; RTAs, falls	Malcı et al. 2025; Zhang 2021
Skull Base	Skull base fractures: 87.5% (fatal), 32.3% (non-fatal)	n=1,260 isolated head trauma (Turkey)	High-energy impacts, falls from height, RTAs, firearms	Malcı et al. 2025; Dreizin et al. 2021
Facial Bones	Mandible ~40%, Zygomatic ~35%, Maxilla ~15%	2,240 patients, 11-year retrospective (NW China)	Road traffic accidents, falls, interpersonal violence	Mao et al. 2023
Vertebral Column	Radiographic prevalence ~20–30% in adults	National & hospital-based cohorts (China, USA)	Osteoporosis, axial loading, falls	Schousboe 2016; Huang et al. 2023
Humerus (proximal)	~60 / 100,000 per year; higher in elderly	National registry data (Europe)	Low-energy falls (elderly), high-energy trauma (young adults)	Iglesias-Rodríguez et al. 2021
Forearm (Radius/Ulna)	CNFS: radius/ulna fractures among the most common; ASIR 404.5 / 100,000 (China)	5,790,636 cases (China, 1992–2021); CNFS cohort	Falls, RTAs; male peak 30–34, female peak 50–69	Zeng et al. 2025; Zhang 2021
Hand	58,849 fractures adults: Phalanges 57.5%, Metacarpals 17.2%, Carpals 5.2%, Multiple 20.1%	CNFS (431,822 fractures)	Falls, direct trauma, occupational injuries	Zhang 2021
Pelvic Ring & Acetabulum	9 / 100,000 per year; ~3% of CNFS fractures	CNFS (512,187 individuals)	Falls (≈55%), MVAs (≈35%)	Chen et al. 2017; Lv et al. 2020; Zhang 2021

Femur (proximal/shaft)	PHFs ~60 / 100,000/year; among most severe long-bone fractures	National & regional epidemiology (Europe, China)	MVAs, high-energy trauma, falls (elderly)	Huang et al. 2023; Zhang 2021
Tibia & Fibula	Tibia/fibula among the most frequent long bone fractures; simple, wedge, and complex types described	CNFS data (~several tens of thousands of cases)	Road traffic accidents, sports, rotational injuries	Zhang 2021; Chen et al. 2017
Foot & Ankle (Tarsal/Metatarsal/Calcaneus)	~35–40 / 100,000 per year; 5–10% of adult fractures	CNFS: thousands of cases; distribution across calcaneus, talus, metatarsals	Falls from height, crush injuries, sports	Zhang 2021; Chen et al. 2017

High energy trauma is inferred for anatomical regions that consistently present in association with vehicular accidents, falls from height or massive compressive force. These include the cranial vault and skull base, which in modern forensic and clinical literature are closely associated with fatal or near-fatal events (Malcı et al. , 2025; Dreizin et al. , 2021), as well as the pelvis and femoral shaft, which are commonly fractured in high-energy blunt trauma and are often accompanied by polytrauma (Huang et al. , 2023; AlTurki et al. , 2019).

Low energy is required to fracture bone of the extremities, tarsal and metatarsal as well as phalanges of the hand fall within this category. Thos event happen through low level falls or domestic accidents without vehicular involvement or any form of high energy mechanisms (Zhang (dir.), 2020). Thes fractures are often reported in outpatient or ambulatory settings and rarely co-occur with major organ injuries.

All remaining skeletal regions, including the scapula, clavicle, vertebral column, humerus, radius, ulna, tibia, and fibula, are provisionally classified as medium-energy trauma indicators. These areas exhibit high inter-individual variability in fracture patterns, often depending on situational context and impact dynamics. Medium-energy trauma encompasses injuries from blunt force, moderate-height falls, and non-fatal collisions, and is supported by consistent incidence levels across emergency department studies and orthopedic registries (Chen et al. 2017; Schnetz et al. 2025; Iglesias-Rodríguez et al. 2021).

The craniofacial region, while often treated separately, also supports this model. Adult maxillofacial fracture series, such as those from Mao et al. (2023), confirm a dominance of high-energy causes (56. 3% from RTAs), though regional variation and forensic context can modulate this interpretation.

Overall, this classification allows for a comparative interpretation of observed skeletal trauma in archaeological populations. The integration of clinical data into this model provides a structured basis for formulating kinetic hypotheses based on lesion location and distribution, to be developed in the following section.

By application of the data and the hypotheses of level of kinetic energy, we can now formulate the hypothesis of the lesions found in the sample of Magny-en-Vexin. While no attempt has been made to chronologically organize the lesions of the same individuals, for SEP 33, each were treated separately.

The skull perforation is localized on the cranial vault on the occipital; we can suppose that it is the result of a high energy trauma. The ulnar fracture from a medium energy trauma and the foot of a low energy trauma.

The ulnar fracture of SEP 20 on the diaphysis is then supposedly from a medium energy trauma.

The overview of the modern epidemiological data allowed a categorization of fractures according to the level of kinetic energy based on the recorded etiology of the traumas. While simplified, the classification allows to formulate hypothesis on the archeological contexts. This classification scheme thus offers a structured bridge between paleopathological observations and their etiological interpretation. It lays the groundwork for the next analytical phase, where lesion distribution and individual trauma profiles will be further contextualized to assess insecurity patterns.

Discussion

The concept

Dual-system diagnostic reasoning in paleopathology

The analytical framework employed in this study draws on dual-process models of clinical decision-making, a very complex model that leads to decision making to treat patients. From These models distinguish between two cognitive systems, the intuitive, rapid response System 1 and the analytical, reflective System 2 (Monteiro et al. , 2020; Pelaccia et al. , 2011). In clinical settings, practitioners can match the original input (context and patient history) to known patterns while System 2 engage in more deliberate reasoning and relies on structured mental "scripts" to process complex or unfamiliar cases. In paleopathology, the absence of an established library of diagnostic scripts poses a unique challenge. Consequently, initial assessments are often based on analogical reasoning, which leads to interpretive bias.

The approach developed here aims to address this limitation by formalizing a hypothetico-deductive method. Lesions are not diagnosed solely by their resemblance to known cases but are instead subjected to a structured set of diagnostic criteria that test their morphological and biological coherence. The criteria-based grid thus functions as a methodological bridge, linking intuitive recognition with systematic validation. The grid and the criteria facilitate hypothesis testing through hypothetico-deductive thinking offering a safeguard against confirmation bias. While this method does not negate the contribution of earlier paleopathological research, it proposed a complementary tool designed to support diagnosis offering transparency and reproducibility so that the diagnostic process can easily be followed by others. Although the criteria themselves remain open to refinement and critique, the diagnostic process becomes traceable and methodologically transparent.

This study builds on previous reflections that explicitly highlighted the dual process nature of paleopathological diagnosis. Mays (2020) proposed a model in which both intuitive (Type 1) and analytical (Type 2) reasoning contribute to diagnosis, stressing the lack of formalized "scripts" in paleopathology and the risk of cognitive biases. The diagnostic grid developed here can be viewed as a way to operationalize this dual process perspective by providing explicit, testable criteria to bridge intuitive recognition and systematic validation.

From formulating to testing hypothesis

A key strength of the grid lies in its ability to distinguish lesions that appear morphologically alike but differ in etiology. Drawing on the concept of diagnostic scripts (Charlin et al. , 2000), the grid provides a framework in which individual observations are contextualized within a broader diagnostic landscape. Each criterion is evaluated for its compatibility with known biological processes, such as the phases of fracture healing. This process could allow the integration of fragments, presenting specific criteria. Although certainty may remain elusive in such cases, the structured evaluation of available features offers a grounded basis for cautious interpretations.

Conservation

Skeletal Integrity and Observational Biases

Preservation quality plays a foundational role in paleopathological analysis. In this study, both the Anatomical Conservation Index (ACI) and the Cortical Surface Conservation Index (CSCI) indicated that the sample was uniformly poorly preserved across the assemblage, with more than half of individuals falling into the lowest preservation categories. Poor preservation directly affects the ability to detect diagnostic features, particularly those requiring continuous cortical surfaces or intact articular geometry. Breaking and surface loss hide both clear shapes and small hints like bone growth or surface changes.

This state of preservation directly influences our observations. Individuals whose bones are better preserved are more likely to show evidence of disease or trauma, even if the actual prevalence of injury was similar across the population. Conversely, severely damaged bones may fail to display pathological traces simply because the key features have been lost. This bias is not only statistical but also interpretive, as it affects prevalence estimates, lesion classification, and the inferred anatomical distribution of trauma. For instance, small bones are both more susceptible to fractures and more prone to poor preservation.

This study focused on the skeletal remains from the Merovingian site of Magny-en-Vexin, not only because of their archaeological significance but also because the collection had previously undergone partial osteological assessment and was accessible for a comprehensive re-examination. Despite notable preservation challenges, the assemblage presented enough analyzable lesions to test a diagnostic framework. The site's chronological and cultural context, combined with the

presence of both well-preserved and degraded elements, offered a valuable opportunity to develop and refine diagnostic criteria under real-case constraints

Impact on Biological Profiling

Preservation constraints also hinder the reconstruction of biological profiles, which is essential to contextualizing trauma. The inability to assess adult age-at-death through established pubic symphysis or auricular surface criteria limited any consideration of senescence-related fragility, such as osteoporosis. Without reliable skeletal markers for advanced age, patterns of age-associated trauma, particularly low-energy fractures of the hip, spine, or wrist, remain undetectable.

Similarly, sex estimation based on pelvic was compromised in several cases, restricting the study's capacity to explore sex-specific injury patterns or biomechanical vulnerabilities. These gaps affect not only demographic reconstruction but also interpretations of risk exposure, occupational stress, or social status as inferred from trauma distribution.

Diagnostic Silence and Incomplete Signals

Some lesions, particularly subtle fractures or non-displaced injuries may leave only ephemeral traces that are erased through taphonomic damage. The diagnostic grid constructed in this study can only operate within the observable spectrum; where preservation fails, so too does the system's sensitivity. Diagnostic silence should therefore not be read as diagnostic certainty. In cases of poor preservation, the absence of observable signs should not be interpreted as certainty but rather as an open question, to be considered with caution in further analysis.

Overall, the limitations imposed by preservation highlight the importance of systematically assessing bone condition. Preservation studies should not be treated as minor side notes but as integral components that shape what can realistically be detected. Future frameworks could incorporate explicit preservation thresholds into diagnostic confidence scales, thereby improving both transparency and interpretive caution.

Pattern Recognition

Morphological Intuition and visual Heuristics

Pattern Recognition is essential before entering the grid. The human brain can visually categorize shapes and texture, and experienced analysts rely on this ability to identify lesions. In

our cases we were interested in the aspect of trauma. The question is which visual characteristics, when carefully described, are appropriate indicators for diagnosing trauma. As in clinical science, morphological intuition can be remarkably accurate especially when supported by repeated exposure. Visual heuristics are thus a valuable entry point for the generation of diagnostic hypothesis.

However, as explained in this study, the justification of the intuition base diagnostic needs criteria. The grid does not merely serve to justify a diagnosis but also to strengthen it. Pattern recognition, however, takes time to develop, and inexperienced observers are particularly vulnerable to misinterpreting pathological expressions, as was demonstrated in the preliminary stage of this study. Pattern recognition is a constant learning process and may already rely on some of the criteria. The interpretative weight of pattern recognition alone remains limited.

Integration into the Framework

The diagnostic framework does not reject pattern recognition but instead embeds it within a more systematic process. Morphological resemblance serves as the trigger for further analysis. Once flagged the lesions are evaluated against the proposed criteria. This dual system allows for a reduction of the influence of subjective interpretation.

In particular, the use of reference cases, the antemortem fracture of SEP 20 and SEP33, provided anchored examples that calibrate the expectations. These cases served as the basis of pattern recognition. With those in mind flagged every lesion that had a similar presentation. The perforation of the cranial vault of SEP 33 or the calcaneonavicular fusion of SEP 42 illustrate how recognition can be informing or misleading. Deeper examination was necessary on how they could both be a presentation of trauma or something different. The screening of every lesion in the sample of Magny-en-Vexin was necessary to compile potential basis for the criteria.

When Pattern Recognition Failed

Some lesions defy intuitive classification. From a subtle deformation to synostosis these presentations of trauma are not instinctively linked to traumatic etiology. However, these were not excluded on the basis that the absence of familiar morphology does not equate to the absence of trauma. Conversely, relying on suggestive morphology without corroborating features risks overdiagnosis. This tension between sensitivity and specificity underscores the need for a structured diagnostic framework.

This underscores the necessity of reserving final diagnosis when multiple criteria align. Pattern recognition is a powerful tool only if it initiates the specific inquiry and does not substitute it. As this study proposes, pattern-based observations should be integrated into a criterion-guided reducing premature conclusion inherent of comparative diagnosis.

Pattern recognition, the equivalent of the clinical system 1 of diagnosis, conserves its value as a diagnostic tool, but its effectiveness is contingent on context and training. However, used simultaneously with a structured inquiry, it enriches diagnostic interpretation. Because of lack of experience in this study more lesions were flagged than what an experienced paleopathologist would have flagged although they ended up being necessary to ensure specificity of the criteria.

Evaluating the Diagnostic Grid

Enhancing Diagnostic Consistency

The proposed diagnostic grid developed here offers a structured approach to detecting skeletal trauma. By translating biological, morphological, and radiographic observations into concrete and testable criteria. It establishes a replicable framework for identifying antemortem fractures. This method improves internal consistency and opens doors to developed grounded script and criteria to strengthen diagnostic and allows comparisons across anthropological remains.

In addition to consistency, the grid adds transparency. Each diagnostic decision is explicitly linked to defined features, which reduces the opacity of the process and facilitates critical evaluation of the diagnosis. Instead of the whole diagnostic being discussed it is criterion by criterion that the diagnostic can be discussed in the idea of this concept being adopted by others. It aligns with broader efforts in paleopathology to standardize diagnostic reasoning and move beyond purely analogical and narrative interpretations. Moreover, the dual system builds a bridge between paleopathology and clinical science offering a share framework for potential interdisciplinary dialogue.

Methodological Limitations and Refinement Needs

Despite its contributions, the grid has several limitations. Chief among them is its dependence on preservation quality. Bones that are fragmented or severely eroded may not preserve enough information to satisfy multiple diagnostic criteria. The grid, in its current form, is tailored

to macroscopic and radiographic features visible on dry bone, but not all samples can be imaged, and radiography is often applied selectively.

A second limitation concerns the weighting of criteria. While this study adopted a convergence-based model, in which confidence increases with the accumulation of positive indicators, it does not yet offer a quantifiable threshold of certainty. Expanding the grid to include confidence levels or probabilistic scoring could improve its diagnostic utility. However, the limited number of confirmed fractures at Magny-en-Vexin constrained any formal calibration or statistical analysis. Nevertheless, the recurrence of specific criteria among confirmed fractures suggests that some features carry stronger diagnostic weight than others and should be prioritized in future revisions.

The current state of the grid is only binary: traumatic or not. Yet, some lesions can present hybrid characteristics, partially healed, remodeled, affected by other pathology. For example, osteomyelitis may develop as a complication of a fractures thus etiologically speaking come from trauma and infection (Ortner, 2019). The framework should evolve to accommodate such complexity. On the same note, there are quite a variety of fractures (see Appendix 1) that were not fully encountered in this study.

Toward Broader Applicability

It is important to emphasize that the diagnostic grid was tested exclusively on the Magny-en-Vexin assemblage. While the criteria were developed with the intention of broader applicability, they remain anchored in the specific preservation conditions, lesion types, and contextual features of this site. Further validation on additional assemblages from different temporal and geographical contexts will be necessary to assess its robustness and generalizability.

The grid's modular structure makes it adaptable beyond the Magny-en-Vexin sample. With adjustments and calibration, it has possible application to different skeletal populations, time periods, and burial contexts. Its utility as a comparative tool across sites is promising. While not definitive, it lays groundwork for a more reproducible, teachable, and clinically grounded approach to diagnosis in trauma analysis. Its theoretical value lies not only in what it is already but what this could become: with broader application both nosological and in other archeological periods.

Biological significance of the criteria

Fracture Healing and Morphological Correlates

The diagnostic criteria developed and proposed in this study are not arbitrary descriptors but rather grounded in the known biology of bone repair. The healing of the fracture is dynamic and is composed of multiple steps from the callus formation to the remodeling (Betts et al. , 2022). Each step involves a change in the bone tissues in order to repair it.

The smooth, localized bone apposition reforming the cortical continuity is a proof that the remodeling has occurred. The rash, and angular deformation, masking the anatomical landmarks indicated that the fracture was not realigned before healing. These fundamental features most strongly reflect the biological response to antemortem trauma in archaeological human remains (and potentially in animals as well). They are also strong because no taphonomic process could be misinterpreted (see Appendix 2).

Positive and Negatives Indicators of Trauma

The criteria proposed include both positive indicators, supporting the diagnosis of fracture if present and not if absent; negative features, exclude the trauma diagnosis if present and support when absent. Positive indicators are those identified in the hypothetico-deductive stage of the diagnostic process, whereas negative indicators are those that halt the process at the stage of pattern recognition by ruling out trauma.

The dual-level approach enhances diagnostic specificity in clinical context. It is the convergence of the multiple criteria that allows confidence in the diagnosis. On the same level, on the proposed system in paleopathology, the presence of positive and negative indicators should put the observer in a caution states. The case of the skull fracture of SEP 33 is the best example, although categorized as an osteolysis, meaning a strong negative indicator that should have stop the diagnostic process for trauma, the evidence of the biophysical process (funnel shape), physiological response (thickening of the inner table, protecting the diploe) points toward a perforating trauma.

Radiographic Correlates and Diagnostic Strength

In addition to macroscopic examination, radiographic imaging reinforces and clarifies morphological interpretations. X-ray and CT imaging allow for the assessment of internal bone structures, including medullary continuity, trabecular architecture, and cortical density. In well-healed fractures, bridging callus tissue typically exhibits a density comparable to the cortical bone and seals the exposed medullary cavity. The presence of a trabecular pattern within the callus suggests physiological remodeling rather than pathological overgrowth (Boyd 2018; Wedel 2013).

Radiographic criteria contribute to the formulation of diagnostic features: although not always pursued as a primary diagnostic tool, radiographic imaging was central in this study to identifying structural signatures of consolidated fractures. Their diagnostic potential remains underexplored on dry bones (Mays 2011). If it is not used systematically, a perfectly healed fracture with subtle macroscopic changes will not be conclusive without a radiography to confirm. The diagnosis of this study was based on a first observation to detect the deformation and associated bone production. When a fracture is properly realigned, no macroscopic deformation may be visible and the callus can remain undetected, but radiography will still reveal it. Moreover, a fragmented bone, a proximal ulna with a complete olecranoid, a diaphysis with a thickening. With a lot of taphonomic artefacts and with only a macroscopic approach we can side on non-pathological or with a trauma trace. The X-ray then shows none of the criteria of the grid therefore with medical imaging we can exclude the trauma diagnosis.

Recent studies highlight just how important this approach is. For example, Schultz (2001) showed how using a combination of macroscopic, radiographic, and histological techniques lets researchers spot subtle changes in bone remodeling. Judd and Redfern (2011) found that radiography can reveal signs of healed fractures hidden beneath the surface. Harvig and colleagues (2012) also pointed out that using radiographic examinations can help tell the difference between trauma and changes caused by natural processes after death or cremation. Altogether, these studies suggest that imaging should be used more widely in paleopathology, not just to double-check findings, but as a key part of diagnosing issues from the start.

In sum, the diagnostic criteria in this study are based on biological processes, supported by evidence, and can be reliably repeated by others. They are coherent with fracture repair, and they

bring together both what can be seen on the surface and inside the bone to help ensure a strong and well-rounded diagnosis.

Differential Diagnosis in Ambiguous Cases

Differential diagnosis in paleopathology is not about arriving at certainty but about mapping the range of reasonable interpretations. It is a process of testing, exclusion and refinement that is essential for dealing with the inherent ambiguity of the archeological record (Ortner, 2011; Mays, 2018).

The Challenge of Ambiguity

Not all pathological signs fit neatly within established diagnostic categories. Some exhibit incomplete features, or essential elements of the skeleton are missing to have certainty. In such cases, the diagnostic process must remain open to multiple hypotheses. Rather than forcing a binary interpretation (traumatic or not traumatic), the principle of differential diagnosis encourages the formulation and systematic comparison of plausible alternatives.

This study encountered several ambiguous cases that illustrate the need for structured diagnostic comparisons. For example, the unilateral calcaneonavicular fusion of SEP 42 lacked remodeling but presented with abnormal articulation. Similarly, the sacroiliac synostosis in SEP 23 could represent trauma, congenital anomaly, or chronic biomechanical stress. Isolated macroscopic osteolytic lesions could also be the sign of a perforating trauma, osteomyelitis, or a lytic tumor like an eosinophilic granuloma.

The role of Radiography and Skeptical Interpretation

In several ambiguous cases, radiographic imaging was essential to evaluate the lesions against the proposed diagnostic criteria. The parietal perforation in SEP 33, although initially suggestive of a perimortem injury, showed cortical thickening and trabecular sealing that fulfill positive indicators of healing, thereby supporting its interpretation as an antemortem trauma. By contrast, the fused tarsal bone in SEP 42 did not present cortical discontinuity or any signs of reactive bone formation, both of which are required criteria for a traumatic origin. In line with this absence of diagnostic features, the calcaneonavicular synostosis of SEP 42 is best interpreted as non-traumatic.

Especially in poorly preserved skeletons, some traumatic lesions may fail to leave recognizable traces. The framework and differential diagnosis developed here favors diagnostic conservatism: where evidence is incomplete or contradictory, a descriptive label is retained rather than an assertive diagnosis. This approach protects against overinterpretation while preserving analytical transparency.

Interpreting Trauma Through Kinetic Hypotheses

From Anatomical Patterning to Energy Inference

The final aim of this study was to bridge the gap between lesion morphology and distribution with trauma mechanisms through the formulation of kinetic hypotheses. Without detailing the precise causality of the injury, the approach classifies injuries according to the likely level of trauma required to produce them. This is based on modern clinical literature, which correlates anatomical distribution and fracture severity with trauma energy levels.

Three broad categories, low, medium and high energy trauma were defined to structure the interpretations. High energy was typically associated with events like Motorize Vehicle Accidents (MVAs), gunshots wound or falls from great heights frequently involve the cranial vault, diaphyseal fracture of the femur, or the pelvis. Medium energy includes localized blunt force trauma, falls. Low energy trauma often is related to repetitive strains, sports injury and tends to manifest on weight bearing bones and the extremities.

Application to the Magny-en-Vexin Sample

Within the assemblage studied, these kinetic categories informed the potential interpretations of confirmed or ambiguous trauma cases. The partially healed cranial perforation in SEP 33, because of its location and injury type was attributed to a high energy event. The radial fracture of SEP 33 and ulnar fracture of SEP 20 are consistent with a medium energy event such has a fall or blunt blow. The calcaneal deformation of SEP 33 may represent a low energy trauma.

This classification makes us see trauma not as a static lesion but as the result of biomechanical processes. It offers a non-specific contextual framework for the life event of the individuals of the sample. Importantly, there is now speculative attribution of intent (violence versus accident) in the absence of cultural or forensic evidence.

Epidemiological foundations and Archeological Adaptation

The kinetic model was constructed using large-scale epidemiological data from clinical studies. These studies consistently show that trauma energy levels are the primary determinant of anatomical injury patterning, more than age or sex alone. While modern clinical populations differ from historical ones in behavior and risk exposure, the mechanical principles of bone failure remain comparable.

By grounding trauma analysis in biomechanical plausibility rather than sociohistorical inference alone, this model contributes a layer of rigor to paleopathological interpretation. It further enables inter-site comparisons by establishing an abstract but reproducible basis for interpreting skeletal damage.

Limits and Prospects

The kinetic approach proposed by this study is not without limitations. It relies on anatomical distribution as a proxy for trauma energy and does not account for individual variation in bone strength, age or comorbidities. Moreover, the absence of soft tissue limits interpretations about posture, direction of impact or exact trauma dynamics. That information is unreachable and will stay in the past.

Nonetheless, it makes a conceptual advance. By prioritizing mechanism over causation, it offers a biomechanically sound and cautious alternative to more speculative trauma interpretation. Future work could refine the type of energy necessary to cause a fracture on bones by using forensic methodology or enhanced integration of archeological or historical data.

Conclusion

This study aims to refine the diagnostic process of skeletal trauma in archaeological contexts by applying a structured, criterion-based approach to the Merovingian assemblage of Magny-en-Vexin. Building on both macroscopic and radiographic observations, the framework developed here moves beyond purely descriptive or analogical methods by introducing a hypothetico-deductive grid that allows for reproducibility and methodological transparency. The analysis demonstrated that certain lesion features, particularly the association of localized angular deformation and focal bone production, are strong positive indicators of antemortem trauma, while other expressions such as synostosis or isolated osteolytic defects remain more ambiguous.

Several limitations must be acknowledged. The preservation state of the sample strongly constrained the range of diagnostic possibilities, with many lesions either obscured or erased by taphonomic processes. In addition, the small number of clearly diagnostic cases restricted the possibility of statistically calibrating the grid. While this study relied on macroscopic and radiographic techniques, further refinement is necessary to improve the identification of trauma in future work.

Beyond methodological refinement, the study contributes to a broader reflection on how trauma should be understood and is aligned with the global effort to harmonize diagnosis and interpretation in paleopathology. By integrating kinetic hypotheses derived from modern clinical epidemiology, trauma is no longer approached as a static lesion but as the outcome of biomechanical stress acting on past individuals during their lifetime. This shift emphasizes process over intent and highlights the need for caution in interpretation in the absence of corroborating contextual evidence.

In perspective, the diagnostic grid proposed here should be tested on different samples from different contexts to be amplified. The clinical variability will be included, and it will give a broader applicability and reliability. Expanding the corpus of comparative cases will also allow for the weighing of diagnostic criteria and introduce probabilities of trauma rather than binary reasoning. Ultimately, the approach developed in this thesis seeks to lay a possible foundation for a more reproductible and transparent framework for trauma analysis in bioarcheology, one that takes into consideration both empirical observation and clinical knowledge while remaining sensitive to the interpretative constraints of the archaeological record.

References

Ahmad Almigdad, Ahmad Almigdad, Ayman Mustafa, et al. 2022. “Bone Fracture Patterns and Distributions According to Trauma Energy.” *Advances in Orthopedics* 2022 (September): 1–12. https://doi.org/10.1155/2022/8695916.

AlTurki, Abdullah A., Khalid S. AlAqeely, Turki S. AlMugren, and Ibrahim S. AlZimami. 2019. “Analysis of Femoral Fracture Post Motor Vehicle Accidents.” *Saudi Medical Journal* 40 (1): 41–44. https://doi.org/10.15537/smj.2019.1.21547.

Aufderheide, Arthur C., and Conrado Rodríguez Martín. 2011. *The Cambridge Encyclopedia of Human Paleopathology*. First paperback edition. Cambridge University Press.

Baten, Joerg, and Richard H. Steckel. 2018. “The History of Violence in Europe: Evidence from Cranial and Postcranial Bone Trauma1.” In *The Backbone of Europe: Health, Diet, Work and Violence over Two Millennia*, edited by Charlotte A. Roberts, Clark Spencer Larsen, Joerg Baten, and Richard H. Steckel. Cambridge Studies in Biological and Evolutionary Anthropology. Cambridge University Press. https://doi.org/10.1017/9781108379830.012.

Bello, Silvia. 2001. “Taphonomie Des Restes Osseux Humains : Effet Des Processus de Conservation Du Squelette Sur Les Paramètres Anthropologiques.” These de doctorat, Aix-Marseille 2. https://theses.fr/2001AIX20654.

Betts, J. Gordon, Kelly A. Young, James A. Wise, et al. 2022. “6.5 Fractures: Bone Repair - Anatomy and Physiology 2e | OpenStax.” OpenStax, April 20. https://openstax.org/books/anatomy-and-physiology-2e/pages/6-5-fractures-bone-repair.

Boyd, Donna C. 2018. “The Anatomical Basis for Fracture Repair.” In *Forensic Anthropology*. John Wiley & Sons, Ltd. https://doi.org/10.1002/9781119226529.ch9.

Charlin, Bernard, Jacques Tardif, and Henny P. A. Boshuizen. 2000. “Scripts and Medical Diagnostic Knowledge: Theory and Applications for Clinical Reasoning Instruction and Research.” *Academic Medicine* 75 (2): 182–90. https://doi.org/10.1097/00001888-200002000-00020.

Chen, Wei, Hongzhi Lv, Song Liu, et al. 2017. “National Incidence of Traumatic Fractures in China: A Retrospective Survey of 512,187 Individuals.” *The Lancet Global Health* 5 (8): e807–17. https://doi.org/10.1016/S2214-109X(17)30222-X.

Dittmar, Jenna M., Bram Mulder, Anna Tran, et al. 2023. “Caring for the Injured: Exploring the Immediate and Long-Term Consequences of Injury in Medieval Cambridge, England.” *International Journal of Paleopathology* 40 (March): 7–19. https://doi.org/10.1016/j.ijpp.2022.07.004.

Dreizin, Sakai O, Champ K, et al. 2021. “CT of Skull Base Fractures: Classification Systems, Complications, and Management.” *Radiographics : A Review Publication of the Radiological Society of North America, Inc* 41 (3). https://doi.org/10.1148/rg.2021200189.

Dutour, Olivier (1958-) Auteur du texte. 1989. *Hommes fossiles du Sahara : peuplements holocènes du Mali septentrional / Olivier Dutour*. https://gallica.bnf.fr/ark:/12148/bpt6k3334782n.

Harvig, L., N. Lynnerup, and J. Amsgaard Ebsen. 2012. "COMPUTED TOMOGRAPHY AND COMPUTED RADIOGRAPHY OF LATE BRONZE AGE CREMATION URNS FROM DENMARK: AN INTERDISCIPLINARY ATTEMPT TO DEVELOP METHODS APPLIED IN BIOARCHAEOLOGICAL CREMATION RESEARCH." *Archaeometry* 54 (2): 369–87. https://doi.org/10.1111/j.1475-4754.2011.00629.x.

Huang, Bo-Xuan, Yan-Hua Wang, Hai-Bo Wang, et al. 2023. "Epidemiology and the Economic Burden of Traumatic Fractures in China: A Population-Based Study." *Frontiers in Endocrinology* 14: 1104202. https://doi.org/10.3389/fendo.2023.1104202.

"ICD-11 for Mortality and Morbidity Statistics." n.d. Accessed May 14, 2025. https://icd.who.int/browse/2025-01/mms/en#435227771.

Iglesias-Rodríguez, Sandra, D. M. Domínguez-Prado, A. García-Reza, et al. 2021. "Epidemiology of Proximal Humerus Fractures." *Journal of Orthopaedic Surgery and Research* 16 (1): 402. https://doi.org/10.1186/s13018-021-02551-x.

Judd, Margaret A. 2008. "The Parry Problem." *Journal of Archaeological Science* 35 (6): 1658–66. https://doi.org/10.1016/j.jas.2007.11.005.

Judd, Margaret A., and Rebecca Redfern. 2011. "Trauma." In *A Companion to Paleopathology*. John Wiley & Sons, Ltd. https://doi.org/10.1002/9781444345940.ch20.

Le Forestier, Cyrille. 2023. *Archéologie des nécropoles mérovingiennes en Île-de-France*. Revue archéologique d'Île-de-France 7e. RAIF.

Lovell, Nancy C. 1997. "Trauma Analysis in Paleopathology." *American Journal of Physical Anthropology* 104 (S25): 139–70. https://doi.org/10.1002/(SICI)1096-8644(1997)25+%253C139::AID-AJPA6%253E3.0.CO;2-%2523.

Lv, Hongzhi, Wei Chen, Tao Zhang, et al. 2020. "Traumatic Fractures in China from 2012 to 2014: A National Survey of 512,187 Individuals." *Osteoporosis International* 31 (11): 2167–78. https://doi.org/10.1007/s00198-020-05496-9.

Malcı, Emir Bayram, Dilek Durak, Vahide Aslıhan Durak, et al. 2025. "Frequency and Pattern of Skull Base and Vault Fracture in Isolated Head Trauma." *Chinese Journal of Traumatology*, May, S1008127525000562. https://doi.org/10.1016/j.cjtee.2025.01.002.

Mao, Jingjing, Xiaojie Li, Kun Cao, et al. 2023. "Epidemiology of Maxillofacial Fractures in Northwest China: An 11-Year Retrospective Study of 2240 Patients." *BMC Oral Health* 23 (313). https://doi.org/10.1186/s12903-023-03006-x.

Martinez-Zelaya, Victor R., Nathaly L. Archilha, Mônica Calasans-Maia, Marcos Farina, and Alexandre M. Rossi. 2021. "Trabecular Architecture during the Healing Process of a Tibial

Diaphysis Defect." *Acta Biomaterialia*, Biomineralization: From Cells to Biomaterials, vol. 120 (January): 181–93. https://doi.org/10.1016/j.actbio.2020.08.028.

Mays, S.A. 2020. "A Dual Process Model for Paleopathological Diagnosis." *International Journal of Paleopathology* 31 (December): 89–96. https://doi.org/10.1016/j.ijpp.2020.10.001.

Mays, Simon. 2011. "The Relationship Between Paleopathology and the Clinical Sciences." In *A Companion to Paleopathology*, 1st ed. Wiley. https://doi.org/10.1002/9781444345940.ch16.

Mays, Simon. 2018. "How Should We Diagnose Disease in Palaeopathology? Some Epistemological Considerations." *International Journal of Paleopathology* 20 (March): 12–19. https://doi.org/10.1016/j.ijpp.2017.10.006.

Monteiro, Sandra, Jonathan Sherbino, Matthew Sibbald, and Geoff Norman. 2020. "Critical Thinking, Biases and Dual Processing: The Enduring Myth of Generalisable Skills." *Medical Education* 54 (1): 66–73. https://doi.org/10.1111/medu.13872.

Myklebust, J. B., F. Pintar, N. Yoganandan, et al. 1988. "Tensile Strength of Spinal Ligaments." *Spine* 13 (5): 526–31.

Ortner, Donald J. 2011. "Differential Diagnosis and Issues in Disease Classification." In *A Companion to Paleopathology*, 1st ed., edited by Anne L. Grauer. Wiley. https://doi.org/10.1002/9781444345940.ch14.

Ortner, DONALD J. 2019. *Ortner's Identification of Pathological Conditions in Human Skeletal Remains*. Elsevier. https://doi.org/10.1016/C2011-0-06880-1.

Pelaccia, T., J. Tardif, E. Triby, C. Ammirati, C. Betrand, and B. Charlin. 2011. "Comment les médecins raisonnent-ils pour poser des diagnostics et prendre des décisions thérapeutiques ? Les enjeux en médecine d'urgence." *Annales françaises de médecine d'urgence* 1 (1): 77–84. https://doi.org/10.1007/s13341-010-0006-1.

Roberts, Charlotte A., and Keith Manchester. 2010. *The Archaeology of Disease*. 3rd ed. History Press.

Ruffer, Marc Armand. 1913. "Studies in Palæopathology in Egypt." *The Journal of Pathology and Bacteriology* 18 (1): 149–62. https://doi.org/10.1002/path.1700180116.

Schnetz, M., A. Wengert, C. Ruckes, T. Jakobi, A. Klug, and Y. Gramlich. 2025. "Open Fractures of the Lower Leg: Outcome and Risk-Factor Analysis for Fracture-Related Infection and Nonunion in a Single Center Analysis of 187 Fractures." *Injury* 56 (6): 112303. https://doi.org/10.1016/j.injury.2025.112303.

Schousboe, John T. 2016. "Epidemiology of Vertebral Fractures." *Journal of Clinical Densitometry* 19 (1): 8–22. https://doi.org/10.1016/j.jocd.2015.08.004.

Schultz, Michael. 2001. “Paleohistopathology of Bone: A New Approach to the Study of Ancient Diseases.” *American Journal of Physical Anthropology* 116 (S33): 106–47. https://doi.org/10.1002/ajpa.10024.

Sirat, J. 1972. “Fouille de sauvetage à Magny-en-Vexin (Val-d’Oise), lors de la construction du collège Claude Monet. Rapport de fouille [Non publié].”

Taupin, Dumont, and Raymond. 1998. “Magny-en-Vexin (Val-d’Oise), collège Claude Monet. Rapport final de fouille archéologique préventive (12/11/1997-15/01/1998).” Service régional de l’archéologie d’Île-de-France / AFAN Île-de-France.

Waldron, Tony. 2009. *Palaeopathology*. Cambridge Manuals in Archaeology. Cambridge university press.

Wedel, Vicki L., ed. 2013. *Broken Bones: Anthropological Analysis of Blunt Force Trauma*. Second edition. Charles C. Thomas, Publisher.

Zeng, Yuan, Minhua Hu, Zhiming Zhang, et al. 2025. “The Incidence, Prevalence, and Health Burden of Forearm Fractures in China from 1992 to 2021 and Forecasts for 2036.” *Frontiers in Public Health* 13 (June): 1566421. https://doi.org/10.3389/fpubh.2025.1566421.

Zhang, Yingze, ed. 2020. *Clinical Epidemiology of Orthopaedic Trauma:
*. Third. Thieme Publishers.

Appendix

Appendix 1: French to English terminology of Trauma

Table 1 Classification of fracture: French to English with definition in French

Français	Anglais	Définition	Références
Fracture simple	**Simple fracture**	Rupture complète d'un os sans déplacement majeur ni fragmentation	Ortner, 2019; Lovell, 1997
Fracture comminutive	**Comminuted fracture**	Os fragmenté en plusieurs morceaux après un impact violent	Wedel, 2013; Lovell 1997
Fracture en bois vert	**Greenstick fracture**	Fracture incomplète, fréquente chez ll'enfant, où un côté de l'os est cassé et l'autre plié	Waldron, 2009; Ortner, 2019
Fracture en spirale	**Spiral fracture**	Fracture due à une torsion excessive sur un os long	Wedel, 2013
Fracture de stress	**Stress fracture**	Microfractures résultant d'une charge répétée sur l'os, souvent invisibles macroscopiquement	Wedel, 2013; Lovell, 1997
Fracture en impaction	**Impacted fracture**	L'os fracturé est enfoncé dans un autre segment osseux	Lovell, 1997; Wedel, 2013
Fracture transverse	**Transverse fracture**	Fracture perpendiculaire à l'axe longitudinal de l'os	Ortner, 2019; Waldron, 2009
Fracture oblique	**Oblique fracture**	Fracture inclinée par rapport à l'axe de l'os	Wedel, 2013; Lovell 1997
Fracture par avulsion	**Avulsion fracture**	Arrachement osseux dû à la traction excessive d'un tendon ou ligament	Wedel, 2013; Lovell, 1997
Fracture par compression	**Compression fracture**	Effondrement osseux souvent observé dans les vertèbres	Ortner, 2019; Waldron, 2009
Fracture par éclatement	**Burst fracture**	Fracture avec enfoncement du disque intervertébral entraînant une fragmentation centrale étendue	Wedel, 2013; Lovell, 1997
Fracture perforante	**Penetrating fracture**	Fracture résultant d'un éclatement de l'os avec un déplacement vers l'extérieur proche du site d'impact.	Lovell, 1997; Ortner, 2019
Fracture articulaire	**Intracapsular fracture**	Fracture impliquant une articulation ou au moins la région métaphysaire	Ortner, 2019
Fracture pathologique	**Pathological fracture**	Fracture résultant d'une fragilisation osseuse due à une maladie préexistante (ostéoporose, infection)	Lovell, 1997; Waldron, 2009

Table 2 Vocabulary of the healing terminology in French to English with definitions in French

Français	Anglais	Définition	Références
Cal osseux primaire	**Primary bone callus**	Formation osseuse désorganisée initiale, visible quelques semaines après la fracture	Ortner, 2019; Schultz, 2001
Cal osseux remodelé	**Remodeled callus**	Réorganisation osseuse après la consolidation, avec remodelage de la structure trabéculaire	Waldron, 2009
Non-union	**Non-union**	Absence de consolidation osseuse, avec persistance d'un espace entre les fragments	Lovell, 1997;
Pseudarthrose	**Pseudoarthrosis**	Formation d'une fausse articulation au site de fracture non consolidée	Waldron, 2009; Schultz, 2001
Ostéite post-traumatique	**Post-traumatic osteitis**	Infection secondaire sur un site de fracture	Waldron, 2009
Réaction périostée	**Periosteal reaction**	Formation d'os sous-périosté en réponse à un stress mécanique ou infectieux	Ortner, 2019; Schultz, 2001

Table 3 Terminology of the deformation related to trauma in French to English with French definitions.

Français	Anglais	Définition	Références
Déformation angulaire	**Angular deformity**	Malunion de fracture entraînant un angle anormal de l'os	Lovell, 1997; Ortner, 2019
Déformation en rotation	**Rotational deformity**	Déviation axiale à la suite d'une fracture mal réduite	Waldron, 2009;
Déformation par raccourcissement	**Shortening deformity**	Perte de longueur osseuse due à un cal vicieux	Wedel, 2013
Déformation en crosse	**Bow deformity**	Courbure excessive d'un os long après un traumatisme en croissance	Ortner, 2019; Schultz, 2001

Appendix 2: Criteria, their significations, and clinical interpretations

Table 4 Link between descriptive criteria and their biological significance.

Macroscopic Criterion	Paleopathological Significance	Equivalent Clinical Interpretation	References
Abrupt linear deformation	Indicates a sharp, angular break typical of acute, high-energy trauma rather than plastic bending.	Non-curved fracture, typical of direct impact.	Lovell, 1997; Waldron, 2009
Localized deformation	Focal distortion suggests a mechanical lesion rather than a systemic condition (e. g. , rickets).	Site-specific trauma.	Ortner, 2019; Lovell, 1997
Cortical discontinued	Clear break in the outer bone layer confirms the fracture; a key sign of antemortem trauma.	Diagnostic fracture sign.	Roberts & Manchester, 2010
Fragment displacement	Misalignment of fragments indicates complete fracture and lack of post-traumatic repositioning.	Displaced fracture.	Ortner, 2019; Aufderheide & Rodríguez-Martín, 2011
Overlapping edges	Superimposition of fragments indicates compressive forces; suggests healing occurred in a misaligned state.	Impacted or shortened fracture.	Lovell, 1997; Roberts & Manchester, 2010
Radiographic criterion			
Fragment conserved cortical integrity	Fragments show intact, undistorted cortices, indicating fracture occurred without plastic deformation.	Acute fracture with clean break; no bowing.	Ortner, 2019; Lovell, 1997
Unifies fragments	Bone healing links fragments together, proving antemortem origin and physiological response.	Callus bridging = bone repair.	Ortner, 2019; Aufderheide & Rodríguez-Martín, 2011
Covers the entire exposed medulla	Endosteal bone seals the medullary cavity, indicating mature internal repair.	Consolidated healing phase.	Waldron, 2009; Ortner, 2019
Exterior density equal to cortical bone	New bone appears as dense as original cortex, indicating final remodeling stage.	Mature lamellar bone.	Ortner, 2019; Lovell, 1997
Spongy in the center	Trabecular regeneration reflects restoration of internal bone architecture.	Functional recovery of structure.	Aufderheide & Rodríguez-Martín, 2011

No medullary invasion observed	Absence of abnormal bone in the canal rules out infection or aggressive bone disease.	Healed, non-pathological fracture.	Ortner, 2019; Aufderheide & Rodríguez-Martín, 2011
Masking of anatomical landmarks	Excess bone production obscures normal morphology; sign of remodeling or excessive calluses.	Seen in unstable or misaligned healing.	Ortner, 2019; Waldron, 2009
Smooth bone production	Regular surface texture suggests organized and non-infectious bone response.	Lamellar bone excludes inflammatory reaction.	Ortner, 2019; Roberts & Manchester, 2010
Bone production limited to the deformation	Healing is restricted to the injured area, ruling out diffuse bone disorders.	Localized trauma response.	Waldron, 2009; Lovell, 1997
Cavity and/or porosity (absent)	Absence of cloacae or pitting rules out osteomyelitis or metabolic pathology.	No chronic infection.	Ortner, 2019; Waldron, 2009

Appendix 3: Overview of the collection with conservation Index and elementary lesions with location

Legend:

ACI = Anatomical Conservation Index (0–25%, 25–50%, 50–75%, 75–100%)

CSCI = Cortical Surface Conservation Index (Classe 1 to 5)

✓ = observed, – = absent, – = indeterminate

R = right, L= left, ↓ = lower, Lx = undetermined lumbar, Tx = undetermined thoracic, MT3 = third metatarsal.

Table 5 Overview of the studied burial of the excavation of 1997-1998 of Collège Claude-Monet, Magny-en-Vexin, France, with the number of the stucture, the ACI (Anatomical Conservation Index) and CSCI (Cortical Surface conservation Index) and the locations of potential elementary lesions

Structure number	ACI	CSCI	Abnormal bone growth	Osteolysis	Deformation	Synostosis
3 US 8 LOT2	0–25	Classe 5	–	–	–	–
3 US 8+US 21 LOT1	25–50	Classe 4	✓ Radius L	✓ Radius L + MT3 R + Rachis (Tx)	–	–
1	0–25	Classe 5	–	–	–	–
2	75–100	Classe 4	✓ Rachis (1Tx+3Lx)	–	–	–
5	0–25	Classe 5	–	–	–	–
6	0–25	Classe 5	–	–	–	–
8	75–100	Classe 4	✓ Rachis (Lx)	–	–	–
9	0–25	Classe 5	–	–	–	–
10	0–25	Classe 5	–	–	–	–
11	75–100	Classe 5	–	–	–	–
12	0–25	Classe 4	–	–	–	–
13	0–25	Classe 4	–	✓ Skull (Frontal R)	–	–
14	0–25	Classe 5	–	–	–	–
15	0–25	Classe 5	–	–	–	–
16	25–50	Classe 5	–	–	–	–
17	75–100	Classe 4	–	–	–	✓ L5+sacrum
18	0–25	Classe 5	–	–	–	–

19	25–50	Classe 5	–	–	–	–
20	50–75	Classe 4	–	–	✓ Ulna L	–
21	0–25	Classe 5	–	–	–	–
22	50–75	Classe 4	–	–	–	–
23	75–100	Classe 4	✓ Tibia L + Fibula L	–	✓ Tibia L	✓ Coxal + Sacrum
24	75–100	Classe 4	–	–	–	–
25	75–100	Classe 4	✓ Rachis (C2+3Tx)	✓ Rachis (C2+3Tx)	–	–
26	0–25	Classe 5	–	–	–	–
27	75–100	Classe 4	–	✓ Rachis (C2+2Tx) + 1 Rib	✓ Skull (Occipital + Parietal)	–
28	50–75	Classe 5	–	–	–	–
29	0–25	Classe 5	–	–	–	–
30	75–100	Classe 4	–	–	–	–
32	25–50	Classe 4	–	–	–	–
33	75–100	Classe 4	✓ Fibula R + Scapula L + Radius R	✓ Parietal L	✓ Tibia R + Calcaneus L + Talus L	–
34	50–75	Classe 4	–	–	–	–
35	0–25	Classe 5	–	–	–	–
36	75–100	Classe 4	–	✓ Skull (Frontal)	–	–
38	0–25	Classe 5	–	–	–	–
39	0–25	Classe 4	–	–	–	–
40	0–25	Classe 5	–	–	–	–
41	0–25	Classe 5	–	–	–	–

42	75–100	Classe 4	✓ Cuneiform L + Rachis (Lx)	–	✓ Talus L+R	✓ Calcaneus + navicular L
43	0–25	Classe 4	–	–	–	–
44	25–50	Classe 4	✓	✓	–	–
45	0–25	Classe 5	–	–	–	–
46	50–75	Classe 5	–	–	–	–
47	25–50	Classe 4	–	–	–	–
48	0–25	Classe 5	–	–	–	–
49	25–50	Classe 5	–	–	–	–
50	0–25	Classe 5	–	–	–	–
51	50–75	Classe 5	–	–	–	–
52	25–50	Classe 5	–	–	–	–
53	75–100	Classe 4	–	–	–	–
55	50–75	Classe 4	–	✓ Skull (Frontal) +	–	–
56	75–100	Classe 4	–	–	–	–
57	75–100	Classe 4	–	–	–	–
59	0–25	Classe 4	–	–	–	–
60	0–25	Classe 5	–	–	–	–
61	50–75	Classe 4	–	–	–	–
62	0–25	Classe 5	–	–	–	–
63	0–25	Classe 4	–	–	–	–
21 LOT 1	0–25	Classe 5	✓ Skull (Frontal + Parietal)	–	✓ Parietals L&R	–
59 ?	0–25	Classe 5	–	–	–	–
59 US 196	75–100	Classe 4	–	–	✓ ↓ Limb R	–

Appendix 4: Medical imaging

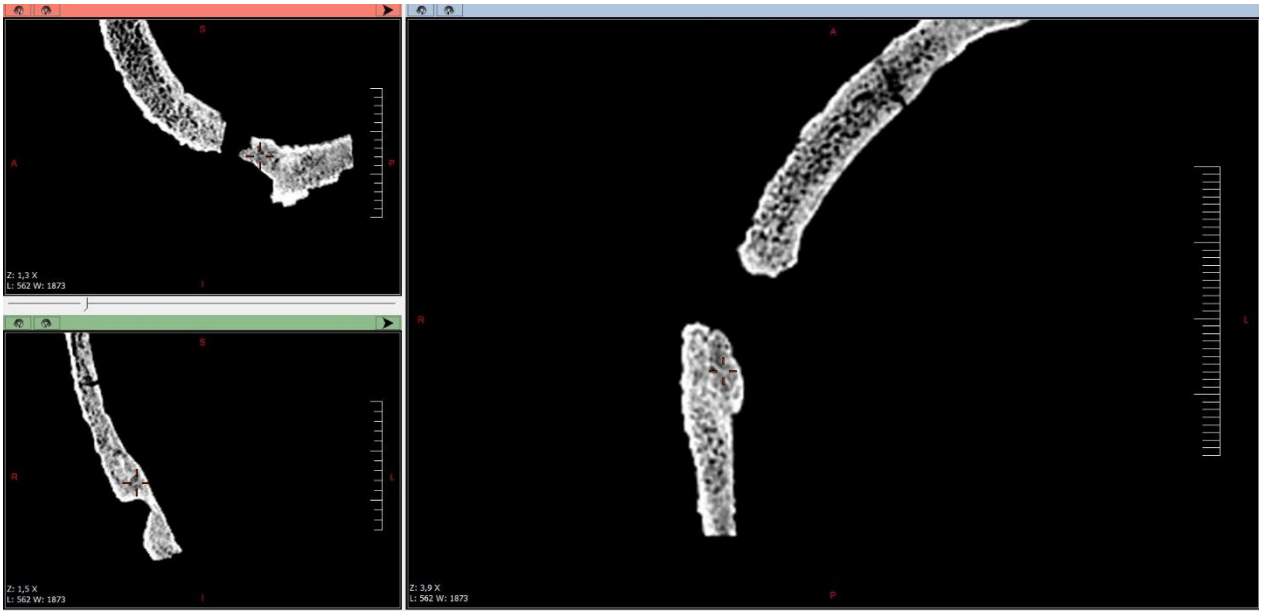

Figure 1 Screenshot of the scanner imaging of the cranial vault of SEP 33, excavation of 1997-1998, Collège Claude Monet, Magny-en-Vexin, France.

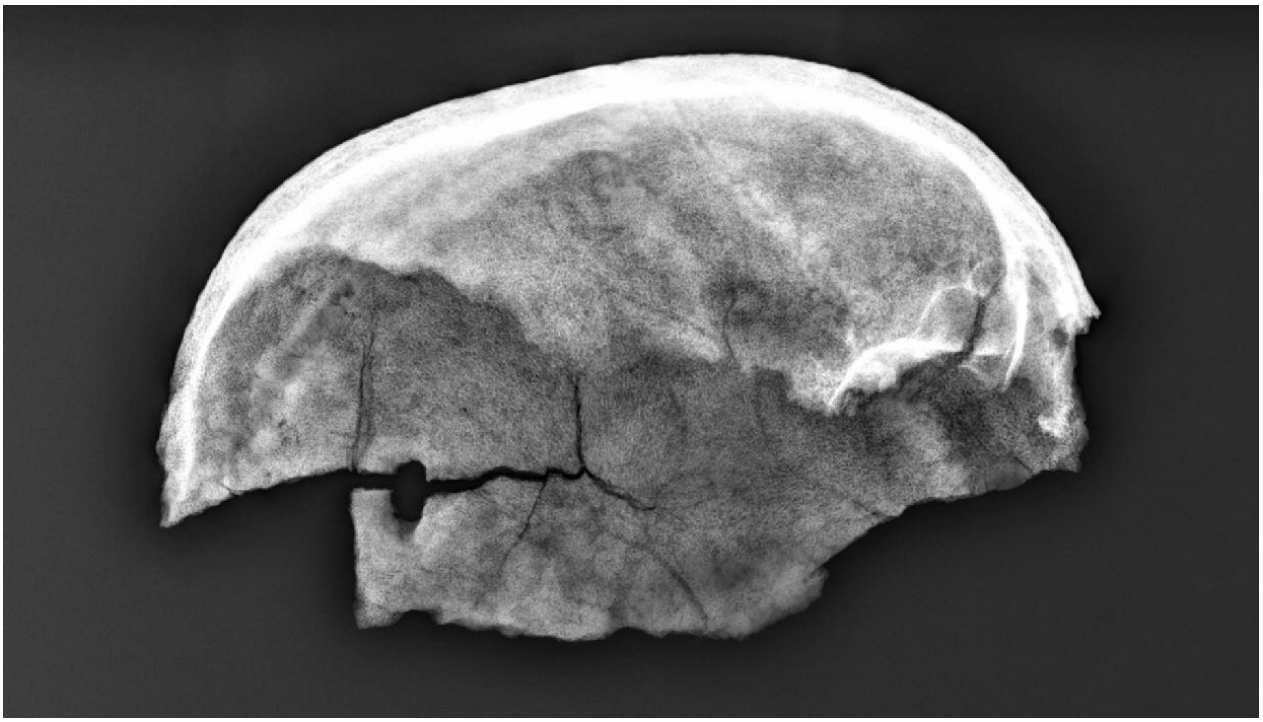

Figure 2 Radiography of the cranial vault of SEP 33 right lateral view, excavation of 1997-1998, Collège Claude Monet, Magny-en-Vexin, France.

Figure 3 Radiography of the left calcaneus of SEP 33 right lateral view excavation of 1997-1998, Collège Claude Monet, Magny-en-Vexin, France.

Figure 6 Radiography of the right radius and right ulna of SEP 33, right vie, excavation of 1997-1998, Collège Claude Monet, Magny-en-Vexin, France.

Figure 5 Radiography of the left ulna of SEP 33 posterior view, excavation of 1997-1998, Collège Claude Monet, Magny-en-Vexin, France.

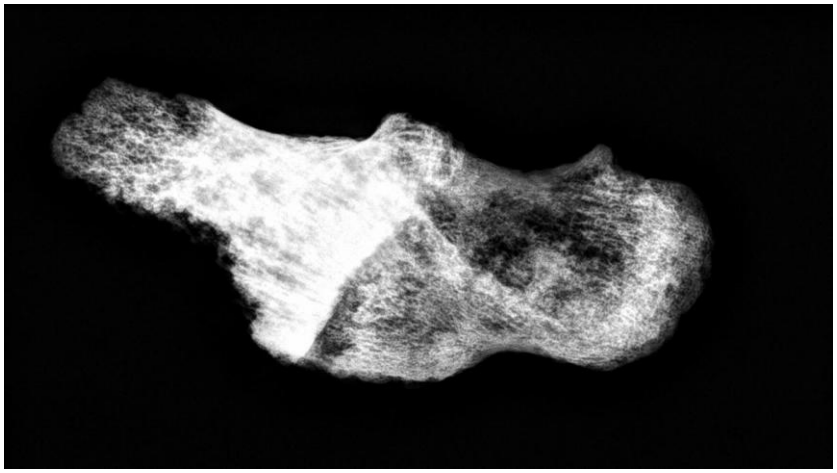

Figure 4 Radiography of the fused right calcaneus with the right navicular of SEP42, superior view, excavation of 1997-1998, Collège Claude Monet, Magny-en-Vexin, France.

Appendix 5: More photography of elementary lesions

Abnormal Bone Production:

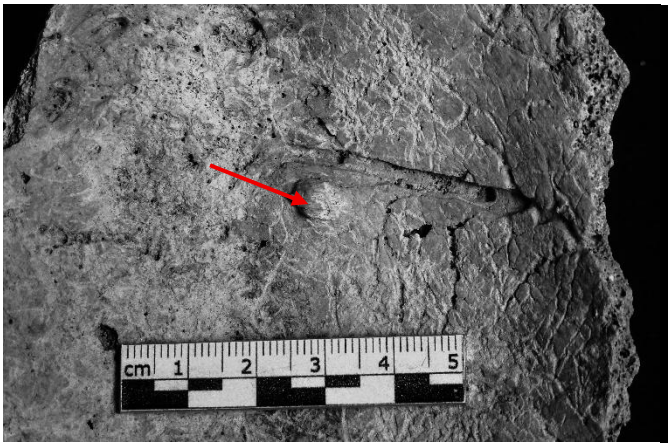

Figure 8 Photography of the inside of the cranial vault of SEP 21 LOT1, presenting an ABP (red arrow), from the excavation of 1998, Collège Claude Monet, Magny-en-Vexin, France.

Osteolysis :

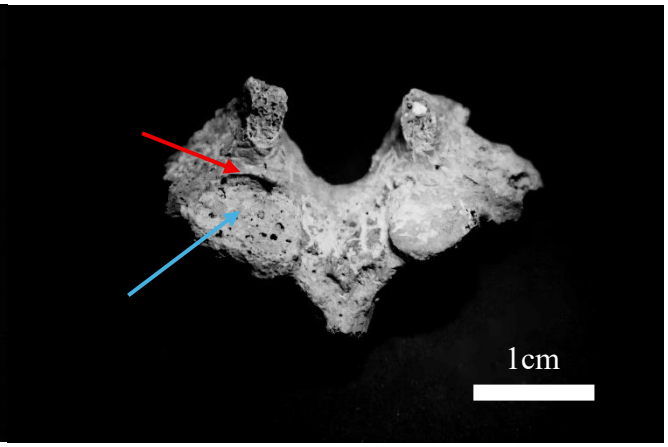

Figure 7 Photography of a thoracic vertebrae of SEP 2, in posterior view presenting some osteolysis lesions (blue arrow) and abnormal bone production (red arrow), excavation of 1998 Collège Claude Monet, Magny-en-Vexin, France.

Deformation:

Figure 9 Photography of the cranial vault of SEP 27, in right lateral view, presenting a deformation (green arrow), burial of 1998, Collège Claude Monet, Magny-en-Vexin, France.

All synostosis of the sample were analyzed.

This thesis focuses on identifying and interpreting antemortem bone trauma in the early medieval necropolis of the Collège Claude Monet in Magny-en-Vexin, Val-d'Oise, France. A total of 62 individuals were studied, considering bone preservation and lesion morphology. The analysis is based on a dual-process diagnostic model derived from clinical medicine. This study develops and proposes criteria for identifying trauma. Macroscopic observations were supplemented by radiographic examinations to add criteria. The analysis shows that localized angular deformation associated with focal bone production constitutes a strong form of recognition. Other lesions, such as osteolysis and synostosis, proved to be less reliable, which justifies the development of more precise criteria. Confirmed cases served as the basis for hypothetical-deductive reasoning. An epidemiological study of modern populations established the basis for kinetic syndrome by linking the anatomical distribution of fractures to presumed energy levels. These results emphasize that this is merely a methodological exploration that exposes the potential and limitations of applying a dual process to paleopathology. This approach promotes transparency and caution in diagnosis and interpretation, paving the way for applications in other contexts.

Ce mémoire porte sur l'identification et l'interprétation des traumatismes osseux, antemortem, dans la nécropole du haut moyen-âge du Collège Claude Monet (Magny-en-Vexin, Val-d'Oise, France). 62 individus ont été étudiés en prenant en compte la conservation osseuse et la morphologie des lésions. L'analyse s'appuie sur un modèle diagnostique à double processus issu de la médecine clinique. L'étude développe et propose donc une grille de critères afin d'identifier les traumatismes. Les observations macroscopiques ont été complété par des examens radiographiques pour éteindre les critères de diagnostic. L'analyse montre qu'une déformation angulaire localisée, associée à une production osseuse focale, constitue une reconnaissance de forme forte. D'autres lésions, l'ostéolyse et les synostoses, se sont révélées moins fiables justifiant le développement de critères plus précis. Les cas certains ont servi de base a un raisonnement hypothético-déductif. Une étude épidémiologiques sur des populations modernes ont permis de poser les bases vers la construction de syndrome cinétique, reliant la distribution anatomique des fractures au niveau d'énergie supposé. Les résultats soulignent qu'il ne s'agit que d'une exploration méthodologique exposant le potentiel autant que les limites d'un double processus appliqué à la paléopathologie. Malgré tout, la démarche renforce la transparence et la prudence dans le diagnostic et l'interprétation et ouvre la voie à des applications sur d'autres contextes.